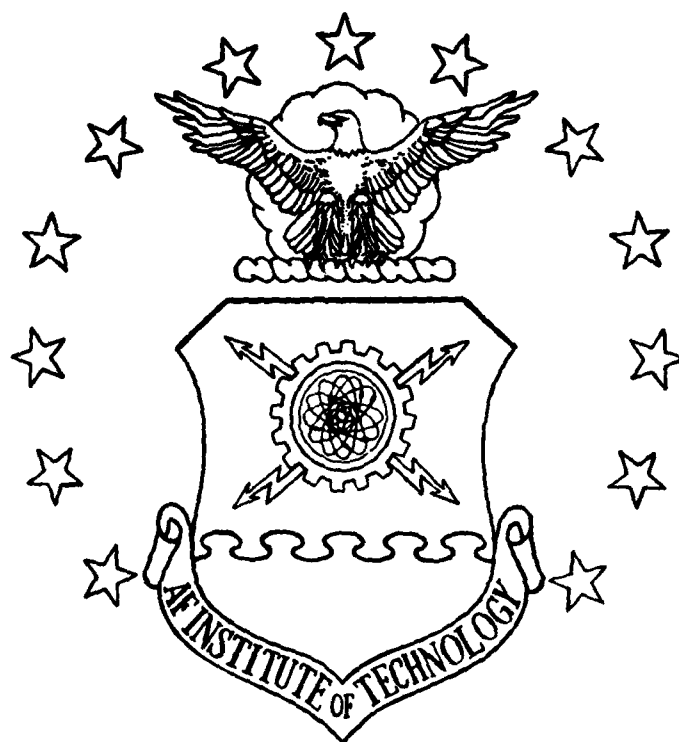MICROCOPY RESOLUTION TEST CHART
NATIONAL BUREAU OF STANDARDS-1963-A

DTIC

AD-A151 897

NULL GENERATION USING DISCS ON A REFLECTOR

THESIS

Michael D. Rudisill
Captain, USAF

AFIT/GE/ENG/84D-55

DTIC
ELECTE
APR 2 1985

A

DEPARTMENT OF THE AIR FORCE
AIR UNIVERSITY
AIR FORCE INSTITUTE OF TECHNOLOGY

Wright-Patterson Air Force Base, Ohio

85   03   13   143

DTIC FILE COPY

AFIT/GE/ENG/84D-55

NULL GENERATION USING DISCS ON A REFLECTOR

THESIS

Michael D. Rudisill
Captain, USAF

AFIT/GE/ENG/84D-55

DTIC
ELECTE
APR 2 1985

A

AFIT/GE/ENG/84D-55

NULL GENERATION USING DISCS ON A REFLECTOR

THESIS

Presented to the Faculty of the School of Engineering

of the Air Force Institute of Technology

Air University

In Partial Fulfillment of the

Requirements for the Degree of

Master of Science in Electrical Engineering

Michael D. Rudisill, B.S.

Captain, USAF

December 1984

Approved for public release; distribution unlimited

i

Acknowledgments

Table of Contents

List of Figures

AFIT/GE/ENG/84D-55

Abstract

It has been shown possible experimentally to produce nulls in the
pattern of prime focus reflector antenna using discs mounted on the dish.
A model of this antenna system is developed to evaluate optimal configura-
tions and ideal performance.

Aperture integration is the method of analysis used. Discs' effects
are modeled as a phase shift on the aperture. No secondary effects, such
as diffraction, are considered.

Based on the model developed, guidelines are presented for antenna
design. Computer code was written to implement the model and a prediction
of an antenna system's performance is presented.

NULL GENERATION USING DISCS ON A REFLECTOR

Introduction

Historical Background

An adaptive antenna system may be viewed as a spatial filter that provides an improved signal to noise ratio (the noise may be any unwanted signal) compared to a conventional antenna. The signal to noise ratio may be improved by either increasing gain in the direction of the desired signal, or decreasing gain (cancellation or nulling) in the direction of the noise.

Adaptive antenna systems have historically been arrays whose outputs are processed by algorithms capable of steering "main beams," nulls, or both. Modern arrays provide excellent performance in a multitude of applications due to the inherent flexibility of a software-driven system.

Arrays, however, have characteristics such as high complexity, weight, cost, low maximum gain, etc., which may render them unsuitable in some situations. Reflector antennas alternately are of simpler construction and offer high maximum gain per unit weight. Therefore, a method of controlling the far field pattern of a large reflector to produce improved signal to noise ratio (by effectively producing nulls in the direction of interference sources) appears to offer a new flexibility to a highly efficient, and widely used, antenna system.

This work was originated by Dr. J. Leon Poirier and Daniel Jacavanco at the Electromagnetic Sciences Division, Rome Air Development Center,

1

Hanscom AFB, Massachusetts. Extrapolating from work on large, flexible reflectors controlled electrostatically to achieve a perfect shape (i.e., parabolic, etc.); they theorized that by distortion of the reflector in the same manner, pattern nulling may be possible. Work by Havens (Havens, 1983) at the Air Force Institute of Technology showed this to be theoretically possible. However, the control problem of a perfect shape, let alone selective distortion, appears to be too burdensome for practical use (Lang, 1982:666).

In the summer of 1983 Jacavanco demonstrated it was possible to produce nulls in the pattern of a rigid reflector by mounting discs on the reflector dish and adjusting their distance from the dish (Jacavanco, 1984c). This method of reflector distortion appears to offer an inexpensive and simply constructed antenna system capable of null generation.

While the technique had been experimentally demonstrated, there was little theoretical basis for the mechanisms producing the nulls. Therefore, this study was undertaken to attempt to develop theoretical background. Ideally this work will produce a means of calculating optimal configurations, bandwidths, etc.

Approach

Aperture integration was selected as the most straightforward technique of analyzing the antenna system with discs mounted on the dish. While it is well-known that this technique is limited in effectiveness to the "vicinity" of the main beam, it is in this area that null synthesis has been shown effective and is of interest.

2

Coordinate System

In order to avoid confusion a standard coordinate system is used throughout this paper. The focal point of the parabolic reflector is defined as the origin with z=0 the focal plane and the antenna located in the z<0 half-space. Spherical coordinates are used interchangeably with rectangular where they are more convenient. Coordinates that refer to the aperture plane (source) will be primed any time there is any ambiguity.

Electric Fields

Equations for the far field electric field generated by an aperture as given by Stutzman and Thiele (Stutzman and Thiele, 1983:383) are

$$E_\theta = j\beta \ \frac{e^{j\beta r}}{2\pi r} \ (P_x \cos \phi + P_y \sin \phi) \tag{1}$$

$$E_\phi = j\beta \ \frac{e^{j\beta r}}{2\pi r} \ \cos \theta \ (P_y \cos \phi - P_x \sin \phi) \tag{2}$$

Since relative, not absolute, field strengths are of interest (relative to main beam gain), Eqs (1) and (2) are simplified:

$$E_\theta \propto P_x \cos \phi + P_y \sin \phi \tag{3}$$

$$E_\phi \propto \cos \theta \ (P_y \cos \phi - P_x \sin \phi) \tag{4}$$

3

Polarization

The choice of polarization convention is not straightforward. As discussed by Ludwig (Ludwig, 1973), no one convention is universally accepted or optimum for all situations. The spherical coordinates for the far field (as in Eqs (3) and (4)), however, cause serious difficulties when attempting to speak practically of co- and cross-polarization in the far field (linear polarization is assumed throughout this paper). Therefore, a simple approach will be used in order to avoid confusion.

Both source and far field patterns will be expressed in rectangular coordinates. The aperture will be defined in the z=0 plane and the far field pattern broken down into x and y components. Admittedly, in the far field the fields will have z components, however these will be small in the area of interest and will not be computed. This component is readily available from the requirement that the total field be orthogonal to the spherical radial unit vector.

This choice of reference polarization has an additional advantage in that it simplifies Eqs (3) and (4). The far field electric field components are now functions of only the like component of the P vector.

$$|E_i|^2 \propto \cos^2 \theta \ \{(R_e[P_i])^2 + (I_m[P_i])^2\} \qquad i = x,y \qquad (5)$$

(Note that the electric field is squared to provide a power measure.)

P-Vector Evaluation

The P-vector used in Eqs (1) and (2) is generated by integration of the electric field over the aperture. The formulation as given by

4

Stutzman and Thiele (Stutzman and Thiele, 1981:426) for a circular
aperture is

$$\int_0^{2\pi} \int_0^a \overline{E}_a(\overline{r}') \exp \{j\beta r' \sin \theta \cos (\phi - \phi')\} \, r' dr' d\phi' \qquad (6)$$

where $\overline{E}_a(\overline{r}')$ is the electric field on the aperture of radius a, (θ, ϕ) are
far field coordinates, and (r', ϕ') are source (aperture) coordinates.

The double integral in Eq (6) presents a problem since the discs
produce discontinuities in the phase of the aperture electric field.
The discontinuities prompt the use of numerical techniques to evaluate
the integral. The method is taken from Abramowitz (Abramowitz and Stegun,
1972:894)

$$\iint f(x,y) \, dxdy = v \sum_{i=1}^{n} w_i \, f(x_i, y_i) + R \qquad (7)$$

where v is the area of the sections of the partitioned surface, the w_i's
are weighting functions given for a particular integration scheme, and
R is the remainder term which will be neglected. Again, since the v
is a constant multiplier on all terms and only relative numbers are of
interest, it is dropped, yielding

$$\overline{P} \propto \sum_{i=1}^{n} w_i \, \overline{E}_a(r_i) \exp \{j\beta r \sin \theta \cos (\phi - \phi_i)\} \qquad (8)$$

Letting

$$\overline{E}_a(r_i) = |E_a(r_i)| \, e^{j\gamma_i} \qquad (9)$$

Euler's formula is used to break $\overline{P}$ into real and imaginary parts yielding

5

$$\text{Re}[\overline{P}] \propto \sum_{i=1}^{n} w_i \left| \overline{E}_a(r_i) \right| \cos \{j\beta r_i \sin \theta \cos (\phi - \phi_i) + \gamma_i\} \qquad (10)$$

$$\text{Im}[\overline{P}] \propto \sum_{i=1}^{n} w_i \left| \overline{E}_a(r_i) \right| \sin \{j\beta r_i \sin \theta \cos (\phi - \phi_i) + \gamma_i\} \qquad (11)$$

Eqs (10) and (11) are the basis for the integration scheme as implemented. Four variables of summation were used--the real and imaginary parts of P_x and the real and imaginary parts of P_y--to sum over the aperture plane for a given θ and ϕ (far field). These quantities, when used in Eq (5), yield a quantity proportional to the magnitude of the electric field squared, which is normalized to the value obtained for $\theta=\phi=0$, yielding a far field power pattern point.

Theory

Antenna Model

The antenna model is a prime-focus parabolic reflector fed by a point source producing a parabolically tapered aperture field. The polarization of the feed is assumed to be linear with the only cross-polar components of the aperture electric field those induced by the reflector dish. The feed is assumed to block a circular area in the middle of the aperture—essentially setting the electric field to zero. No direct radiation from the feed is considered.

The disc's effect on the aperture field is modeled as a phase shift across a circular projection of the disc on the aperture plane (see Figure 1). Amplitude variation in the field due to the different path lengths is not taken into account. The phase shift of the aperture field is estimated two-dimensionally, as shown in Figure 2, by computing the distance from $F-D_i-A_i$, and subtracting it from twice the focal distance of the dish (the normal path length from the feed to the aperture plane).

Two approximations that are made here are worth mentioning. First, the ray tracing approach used does not take into account the actual geometrical optics path from the disc to the aperture plane. All rays reflected off the disc are assumed to travel on a path normal to the aperture plane—thus, the spreading from the disc is not accounted for.

Second, the disc model is two-dimensional and does not take into account the curvature of the disc in the third dimension. Thus, the phase shift has minor errors except on the radial line running through the center of the disc. In both cases it is assumed the errors introduced are minor for discs which are relatively small in relation to the disc.

7
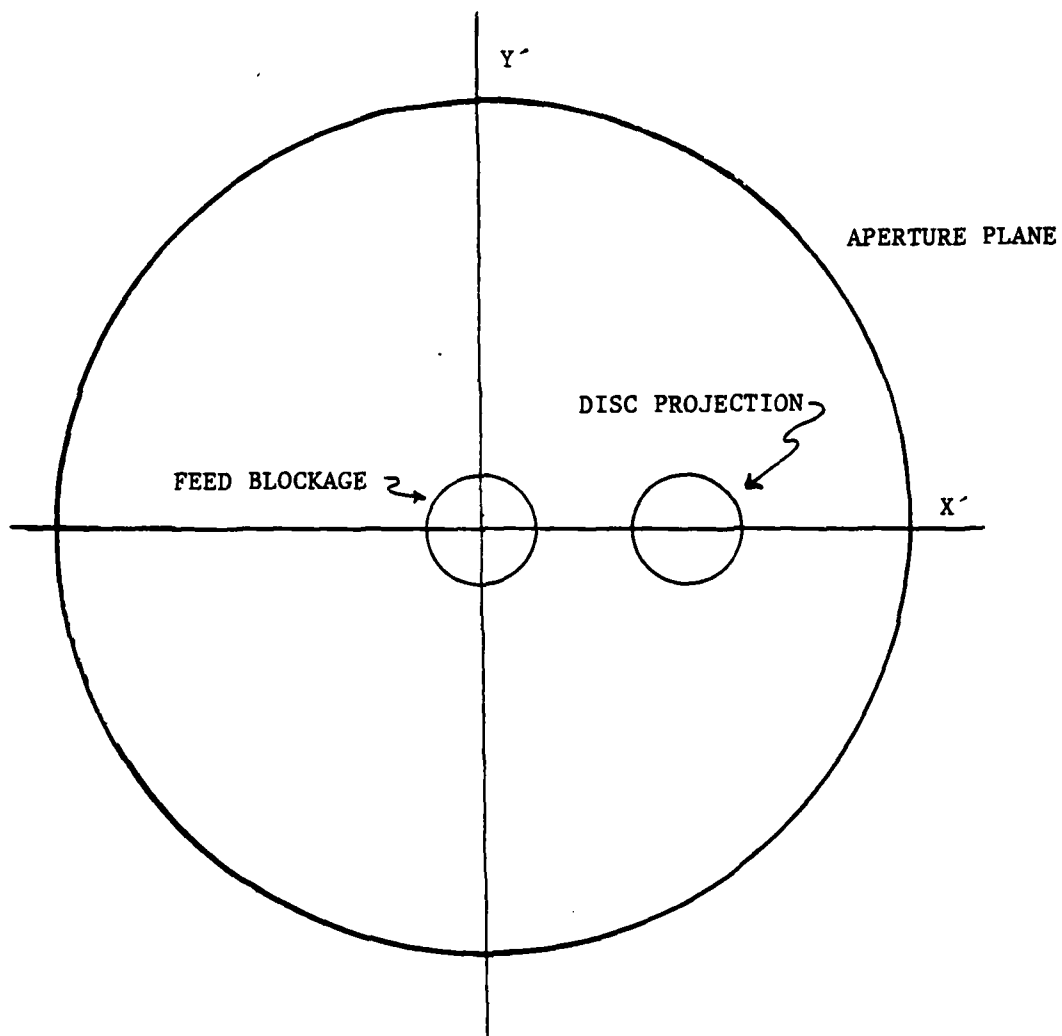
Figure 1. Aperture Plane

8
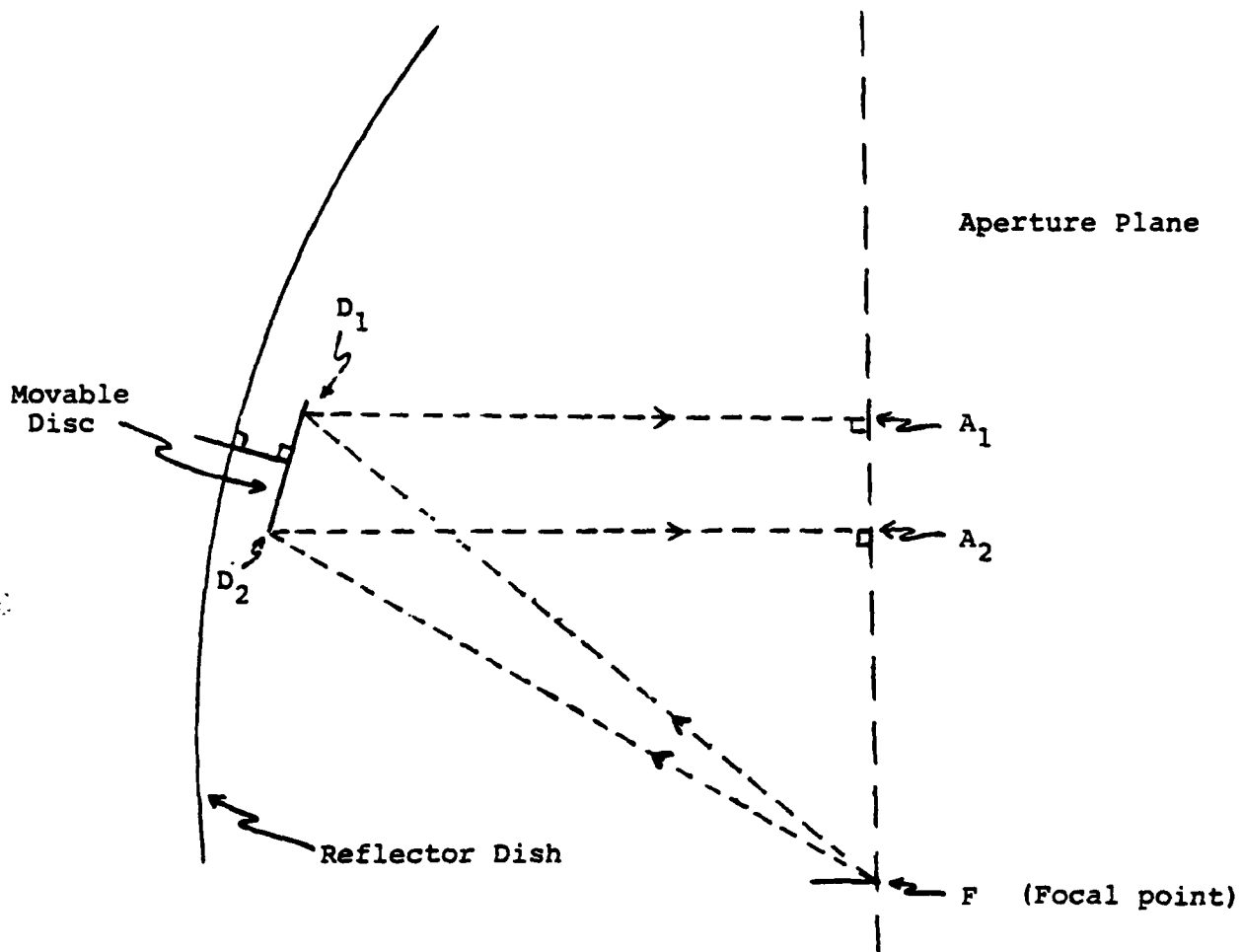
Figure 2. Disc Model

9

Results

This method of breaking down the aperture integral produces simplified
equations that allow insight into the effects produced by the discs and
methods to control these effects. Eq (5) shows that the co-polar pattern
depends only on the P vector component of the same polarization. Thus,
only two of the four variables summed over the aperture plane control
the co-polarized pattern strength. The two variables of interest are

$$\text{Re}[P_j] = \sum_i w_i \left| E_j(r_i) \right| \cos \left[\beta r_i \sin \theta \cos (\phi - \phi_i) + \gamma_i \right] \qquad (12)$$

$$\text{Im}[P_j] = \sum_i w_i \left| E_j(r_i) \right| \sin \left[\beta r_i \sin \theta \cos (\phi - \phi_i) + \gamma_i \right] \qquad (13)$$

where j is the co-polarized unit vector and i references the points being
summed. With no discs present let $\gamma_i = 0$ for all i and examine the magnitude
of the P_i's. The magnitude of the aperture electric field is assumed
to be a function only of the radial position on the aperture plane. Letting
radial position on the aperture plane (r_i) equal a variable number of
wavelengths, k, and solving for the maxima, minima, and zeroes of the
modulation produces

$$k = \frac{n}{4 \sin \theta \cos (\phi - \phi_i)} \qquad n = 0,1,2,\ldots \qquad (14)$$

For a four-foot aperture at a frequency of 2.8 GHz, a plot of the
lines of the maxima, minima and zeroes for the (a) cosine and (b) sine
terms is shown for $\phi=0$ and $\theta=10°$ in Figure 3. Figures 4 and 5 show a plot
of the modulation (an electric field of unit amplitude uniformly over

10
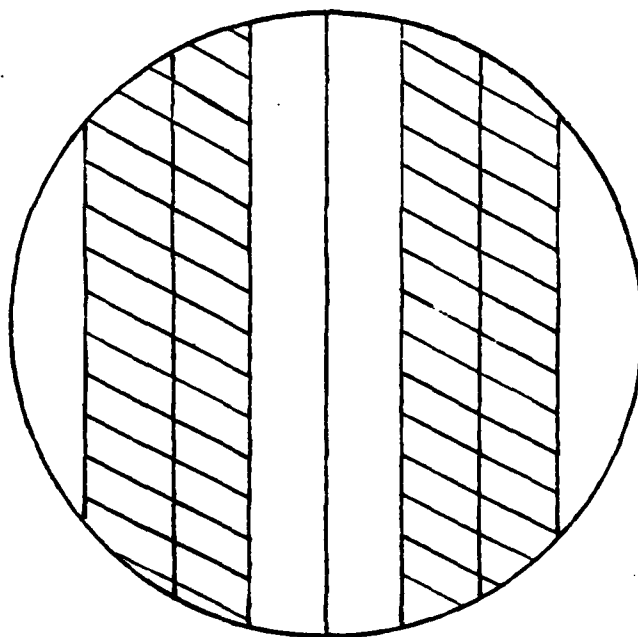
(a)
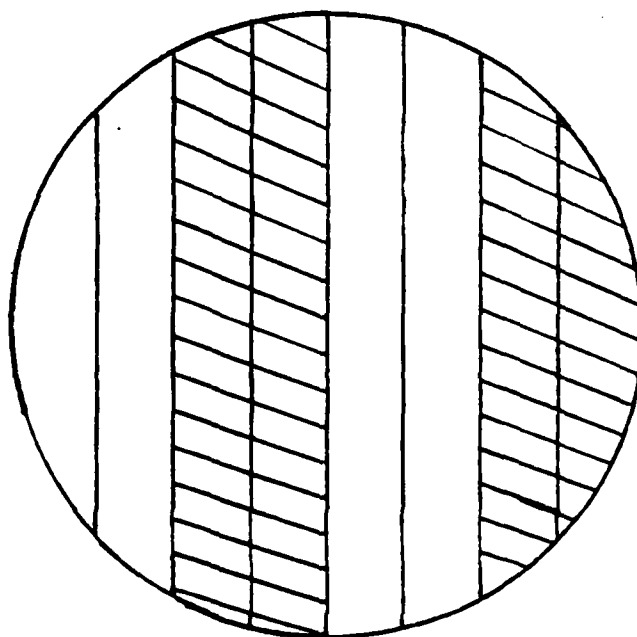
(b)

Figure 3. Sinusoidal Modulation of Aperture
(Hatched areas are negative values)

11
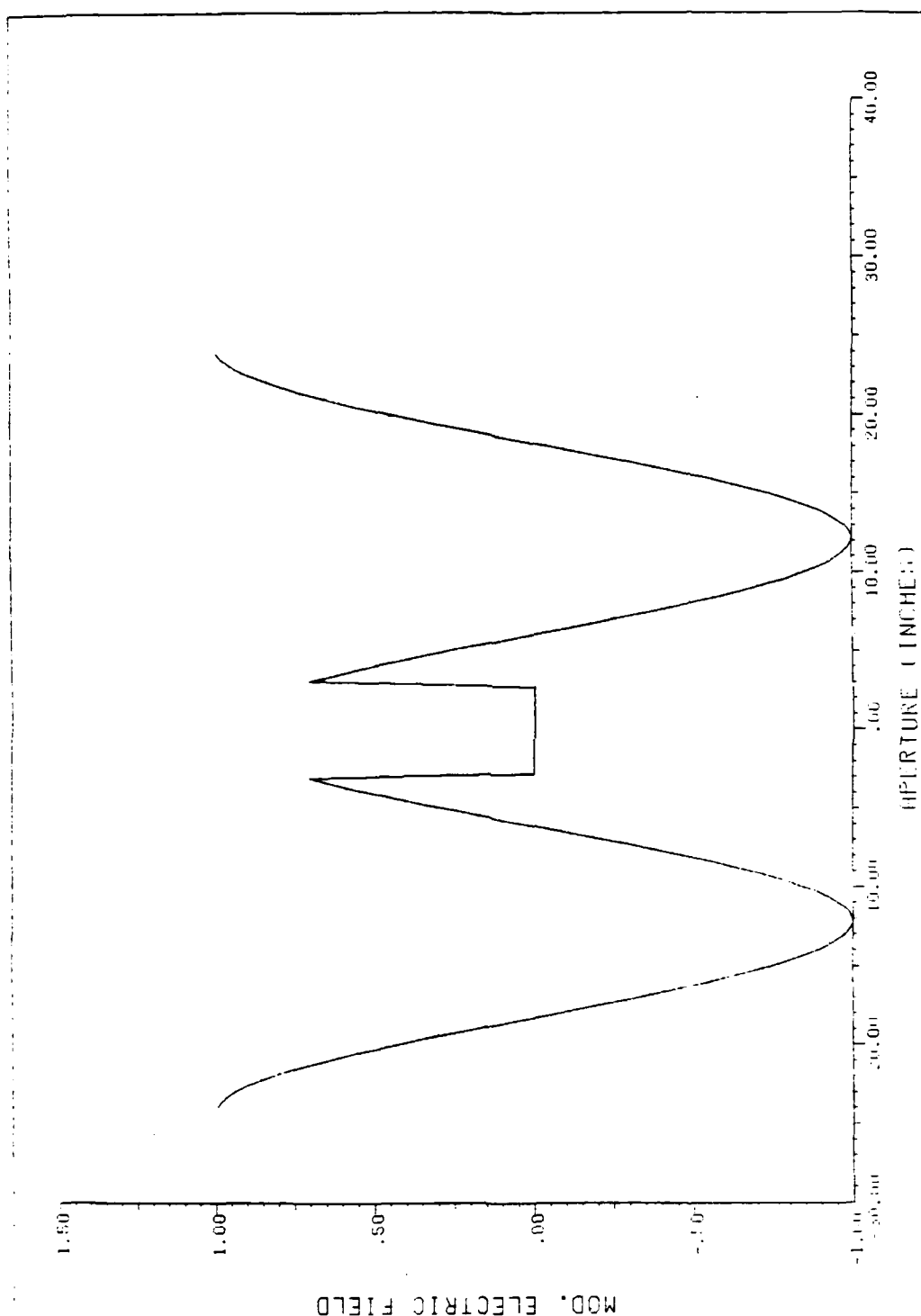
Figure 4. Cosine Modulation on x-Axis of Uniform Aperture at θ=10°

12
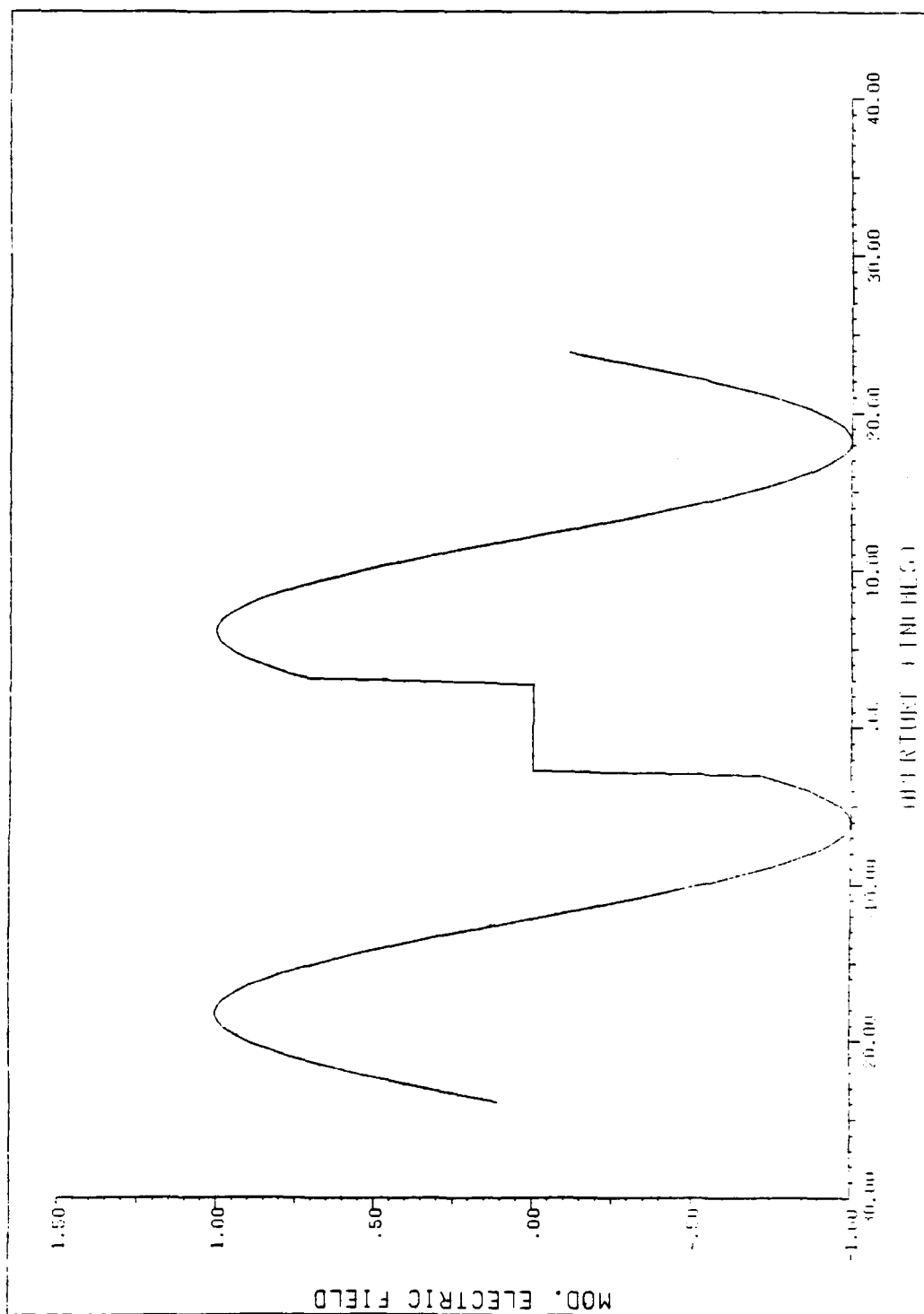
Figure 5.   Sine Modulation on x-Axis of Uniform Aperture at θ=10°

13

the aperture is assumed with a six-inch feed blockage) taken along the x-axis of the aperture. This shows that the imaginary part of the P_i's components are odd-symmetric about the center of the aperture plane. This results in the sum of the imaginary part of the P component equaling zero under all undisturbed conditions, where undisturbed is defined as a perfect reflector with no discs. Note also that the cosine term in the denominator of Eq (14) causes the zones to be perpendicular to the $\phi'=\phi$ line, thus the zones rotate with choice of far field ϕ.

The real part of the P component therefore controls the pattern entirely in the undisturbed case. As θ goes to zero, k goes to infinity allowing the summing of the unmodulated electric field over the entire aperture plane. As θ increases (from zero) the cosine term increasingly modulates the electric field until the sum of the positive and negative sections reaches a minimum, producing the first null. As θ further increases, the magnitude of the sum of the P components increases until the maximum of the first sidelobe. Figure 3 is approximately the maximum of the first sidelobe for aperture distribution shown. The sum continues to oscillate as θ increases, producing the characteristic pattern. The cosine squared term in Eq (5) has been neglected. Its contribution, however, is minimal in the ranges of interest (3 dB at 45°).

Using this simplified model the effects of the discs can be examined. The discs in the model produce a phase shift and it is easily seen how this may cause nulls. Dominant zone is defined as a zone in which the modulated electric field is the same sign as the sum over the entire aperture. By locating the disc in a dominant zone such that it produces a 180° phase shift in the modulated field, the area affected by the disc

14

will effectively change signs. If the disc is the right size, this will cause the sum of the modulated electric field (the real part of the P_i) to equal zero. A larger disc with slightly less (or more) than exactly 180° phase shift may modulate the electric field to produce a zero sum.

The zeroing of the real part of the P_i, however, creates a problem since the symmetry of the sine-modulated electric field (the imaginary part of P_i) has been destroyed--thus creating a non-zero sum. This explains why it requires two discs to produce a null in the pattern. In Jacavanco's original demonstration of this procedure he used two discs on the same side of the aperture (Jacavanco, 1984a). However, this model shows the "optimum" disc placement in terms of using the smallest discs for minimal disturbance of the overall pattern, as symmetric with respect to the center of the dish on the $\phi´=\phi$ line. Using this placement, the imaginary part of the P_i's regain their symmetry and once again sum to zero, producing a zero overall sum and a null in the pattern.

The above discussion overlooks one problem that is easily solved but requires mention. Even the simplified disc model used here does not produce a constant phase shift over the area affected. (The same problem arises using over-sized discs adjusted to less than one-half wavelength phase shift.) This lack of an exact one-half wavelength phase shift is not a problem in zeroing of the real part of the P_i. However, even with symmetrically placed discs as described above, a non-symmetric phase shift again causes a non-zero imaginary part of P_i. A solution is easily obtained by slight adjustment of the phase shift produced by the discs to produce a zero imaginary and real part of the P component (providing the discs are large enough).

15

Dominant Zones

The sign of the sum of the modulated electric field (real part of
the P component) determines which of the zones (positive or negative)
on the aperture dominate. Thus, by appropriate phase shifting (and thus
changing sign) over a portion of the dominant zone, nulling may be accom-
plished. Unfortunately, the determination of whether the sum for a given
far field point is positive or negative is not straightforward.

If there is no blockage for the feed, the sign of the sum alternates
at each sidelobe. The area of zero electric field caused by the feed
blockage, however, destroys this simple property and requires a more
rigorous approach.

The feed blockage may be viewed as a negative electric field super-
imposed on the aperture in the blocked region, thus effectively producing
zero electric field. This results in a far field pattern that is the
superposition of two Bessel functions (Silver, 1949:191). The first
function is positive with a narrow main beam associated with the entire
aperture: the second is negative with a very broad main beam associated
with the blockage. Note that the Bessel function is the analytic counter
to the sum, therefore where the Bessel function, or sum of Bessel functions,
is positive, the sum is positive, and where it is negative, the sum is
negative. In the main lobe, the positive Bessel function dominates,
and the sum is positive. However, the main lobe of the small aperture
(the negative pattern produced by the negative electric field, or blockage),
while small in comparison to the main lobe of the large aperture, may
not be small in comparison to the sidelobes of the large aperture. Thus,
over the area outside the main lobe of the large aperture, but within

16

the main lobe of the small aperture (the blockage), the sum still

oscillates but remains negative due to the dominance of the smaller

aperture. (Note that this analysis is predicated on approximating the

aperture distribution as parabolically tapered--see Silver.)

Disc Placement

There are two methods of determining the dominant zones of a given

far field point. The aperture distribution may be approximated and the

sign of the sum determined analytically as just described, or, a computer

analysis, such as the one in the appendix, may be run and the sign of

the sum determined.

Once the dominant zones are determined the question of in which

zone, and where in the zone, to place the discs arise. If the aperture

distribution is not tapered, the answer is apparent by looking at

Figures 3, 4 and 5. A disc centered in any dominant zone (centered in

the horizontal sense, as shown) will couple the same amount of power

and thus produce the same result. However, when a tapered aperture distri-

bution is considered (as almost all realistic distributions are) another

factor must be considered. Obviously, the closer to the center of the

aperture the disc is located the more power is available. The taper,

therefore, makes the dominant zone closest to the center of the aperture

the optimum for disc placement. The disc should be centered vertically

(see Figure 3) in the zone (again, the closest available position to

the center of the aperture). The horizontal position of the disc in

the zone will not be centered, but slightly offset toward the center

of the aperture due to the taper. Compare Figures 4 and 5 with

Figures 6 and 7. These figures are all the same aperture and far field

17

point, with the only difference being Figures 4 and 5 represent a uniformly illuminated aperture and Figures 6 and 7 represent a parabolically tapered aperture distribution on a 20 dB pedestal. No easy solution for optimum horizontal placement has been found. A good approximation is to center the disc at the maximum of the modulated electric field (taking into account both the tapered electric field and sinusoidal modulation).

Disc Size

While disc placement is somewhat straightforward, the required disc size is not. The required size depends on (1) depth of null required (amount of cancellation), (2) aperture distribution produced by the feed, and (3) disc placement.

The depth of the null or cancellation is directly proportional to the required disc size. Any size disc properly placed will produce some cancellation. In this paper the depth of null desired will be assumed to be the noise floor. For plots and computer simulations, 80 dB below the undisturbed main beam gain will be the assumed noise floor. Therefore, the size of the discs will be proportional to the undisturbed pattern level. Enough power must be coupled by the discs to cancel the undisturbed pattern.

The aperture distribution will have a strong effect on the required disc size. The amount of energy coupled by a given disc is controlled by the energy density incident upon it. For a highly tapered distribution, the energy density is very high near the center of the aperture and thus a smaller disc near the center of the aperture can couple as much energy as a larger disc in the same place with a less tapered distribution.
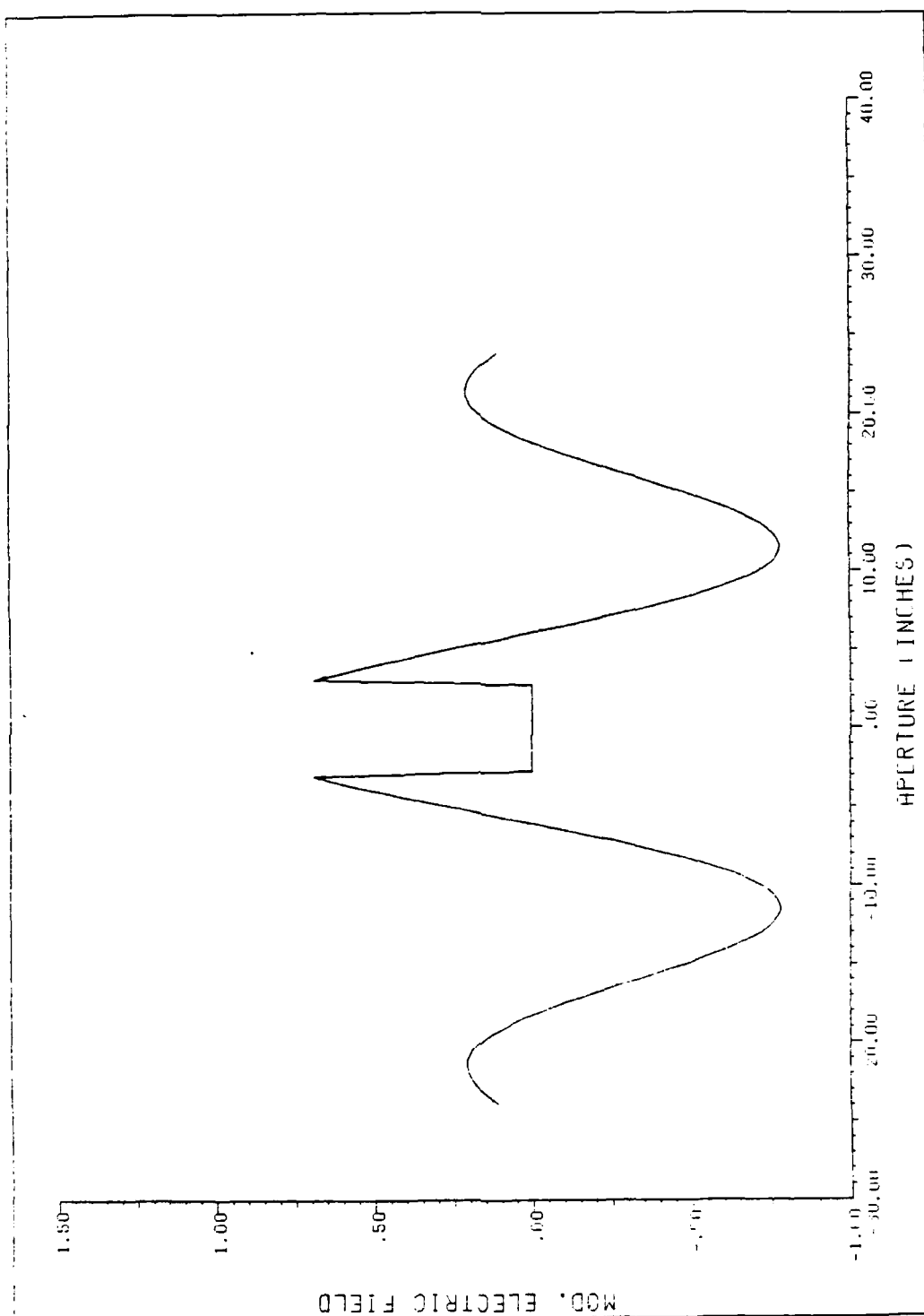
Figure 6.   Cosine Modulation on x-Axis of Tapered Aperture at θ=10°

19
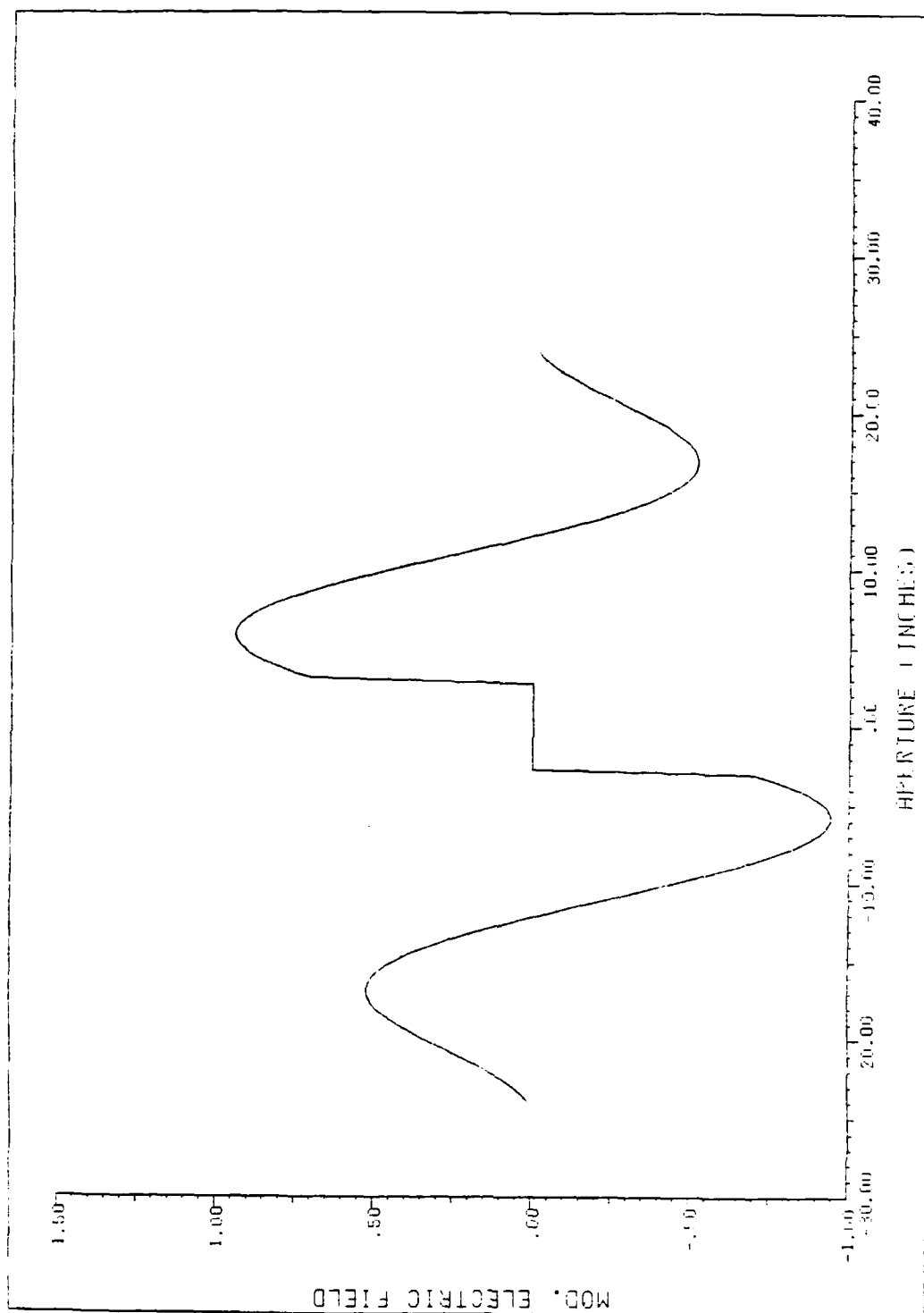
Figure 7. Sine Modulation on x-Axis of Tapered Aperture at θ=10°

20

The effect of disc placement on required size may be broken into two parts. The first follows from the preceding paragraph. If the aperture illumination is tapered, the closer to the center of the aperture the disc is placed the more energy it will couple for a given disc size (of course, the disc must be in a dominant zone to produce any cancellation). As discussed in the previous section, disc placement in the zone also plays a part. Due to the sinusoidal modulation, more apparent power is available near the center of the zone than at the edge.

Performance of an Arbitrary Disc System

All discussion to this point has assumed that the discs used were small enough, and placed correctly, to be contained in a single zone. In practice this may not be the case. The position of the desired null may not be known prior to antenna design, or it may be desired to move the null during operation. The question is then the capability of a given disc system (size and location) to produce a null at an arbitrary point. This is similar to the question discussed in the previous section. The difference is that the disc may not be entirely in one zone, thus adding another complication.

The capability to produce cancellation is governed by the (1) illumination or energy density incident on the disc, and (2) where the disc is located in the zones at a given angle. (If the disc is not in a dominant zone it may not be able to produce any cancellation--only gain.) If the disc spans more than one zone, the area of the disc capable of cancellation is reduced, as the area in a non-dominant zone effectively cancels area in the dominant zone. This is not one-to-one: the effective cancelled area will depend on relative illumination and phase shift produced by the disc.

21

An analysis of an arbitrary disc system follows a two step process. The first involves determing the discs' position in the zones produced by the desired location of the null in the far field. The second step is calculation of the effective area of the discs. The effective area of the disc system (area of the disc system that is not cancelled by an equivalent area in a non-dominant zone) directly controls the amount of cancellation available.

For an aperture with a uniform illumination, effective area may be roughly approximated by the disc's physical area in a dominant zone(s) minus that area in a non-dominant zone(s). This approximation involves estimating the effect of the modulation as a factor of one-half and cancelling this with the factor of two available from the disc's ability not to just zero an area's contribution (to the sum), but to produce a negative of that contribution. If the undisturbed pattern is x dB below maximum pattern gain, an effective area of the aperture may be considered to cause the pattern level by the relationship.

$$x \cong 10 \log_{10} \frac{A_e^2}{A_a^2} \qquad (15)$$

where A_e is the effective area, causing the pattern level, and A_a is the total area of the aperture. An effective disc area equal to the effective area producing the sidelobe is necessary to produce a null. Therefore, the minimum total effective disc area (A_d) is

$$A_d = A_e \cong 10^{(x/20)} A_a \qquad (16)$$

Unfortunately, when a realistically tapered aperture field is considered this approximation breaks down and a more rigorous approach is required (a numerical evaluation will be necessary for most distributions).

22

Effects of a Non-Ideal Antenna

All discussion up to this point has assumed an ideal antenna analyzed using only geometrical-optics "modes." While this approach certainly simplifies the model to a reasonable level of complexity, questions arise as to the validity of certain assumptions. Therefore, a short discussion of these assumptions, and their effects, follows.

Aperture Integration and Geometrical Optics. Aperture integration is an inexact analysis only to the point that (1) not all radiation from the antenna passes through the chosen aperture, and (2) the actual fields in the aperture are not accurately determined. The solution for the first problem is to choose the appropriate aperture such that the far field pattern in the area of interest is accurately determined. For reflector antennas it is well-known that the "ray-optics" aperture used in this model gives acceptable results within 45°-60° of the main beam (Silver, 1949:158).

The use of the geometric optics field in the aperture is obviously an approximation. While this field is present, there are many other contributors to the total field--scattering from feed supports, direct radiation from the feed, and diffraction from the edge of the dish. The assumption made here is that these fields are small in comparison to the geometric optics fields and, in any case, are subject to cancellation by the discs in the same manner as the geometric optics field.

Effects of Reflector Imperfections. One of the major problems with reflectors of this type is the degree to which the reflector dish actually conforms to a parabaloid of revolution. This model represents a perfect surface; however, realistically many reflectors of this type may have substantial errors.

23

The effect of distortions of the surface may be modeled in Eqs (12) and (13) as an additive term on the argument of the sinusoids. The effect is to shift the zones on the aperture. If the distortion is very small (in terms of a wavelength), the effect may be disregarded. However, if the distortion is a significant fraction of a wavelength, the effect of the actual dish geometry must be considered in any analysis. A distortion of one quarter wavelength will cause a phase shift of 180° and thus a total reversal of the zone.

Idealized Feed. The effects in an actual antenna system of having a non-ideal feed may be separated into two parts. The first is extraneous radiation from the feed. This is considered in the previous section concerning the additional fields in the aperture not due to geometrical optics.

The second point is that a feed may not produce an aperture distribution that is parabolically tapered. A review of the analyses will reveal that although this distribution is selected as mathematically convenient, in terms of nulling, the distribution's effect is limited to power available at a given point on the aperture. Thus, while the actual aperture taper may affect required disc size, and optimum disc placement, it has no effect on the basic mechanism of nulling.

Computer Analysis

The equations of the preceding chapter were used to write Fortran
code to evaluate the effect of the discs on the far field pattern of
a reflector. This code was used to test the model's ability to actually
produce nulls in the far field pattern and investigate properties of
the system. The code and a brief explanation of its use is in the appendix;
no attempt will be made to explain its working here.

System Modeled

The antenna modeled is a four-foot diameter parabolic reflector
with a focal length of 27 inches. It operates at 2.8 GHz and is fed
to produce a parabolic aperture distribution (order one) on a 20 dB pedestal.
The feed polarization is assumed to be purely linear (y). This produces
an aperture distribution of the same polarization except as corrupted
by the dish (Stutzman and Thiele, 1981:427). The feed blockage is assumed
to be a six-inch diameter circle at the center of the aperture. These
parameters were chosen to model a generic antenna.

Two disc systems are modeled. The first (disc system I) has two
seven-inch diameter discs symmetrically centered 9.5 inches from the
center of the aperture on the x-axis of the aperture plane. The second
(disc system II) has 2.5-inch discs similarly placed, but centered 4.5
inches from the center of the aperture plane.

These two disc systems were selected because they demonstrate not
only the systems' ability to produce nulls, but also the range and limita-
tions of this system. Note also that the discs do not overlap and thus
could both be mounted on the dish simultaneously to enhance system flexibility.

Radiation Patterns

All the radiation patterns shown are H-plane patterns. The reason
for this choice is that both disc systems are optimally placed to produce
nulls in the $\phi=0$ (H) plane. (The preceding chapter explains the reasons
a disc system symmetrically placed across the center of the aperture
on the $\phi'=\phi$ line is optimum.)

The first pattern shown (Figure 8) is the radiation pattern produced
by the antenna with no discs mounted. This is shown for two reasons.
The first is to demonstrate that the code used will accurately implement
the equations of chapter one. The radiation pattern of the antenna without
the discs may be solved analytically, and the agreement between the analytic
solution and the numerical solution shown is excellent (within .1 dB).
The second reason for Figure 8 is to provide a baseline for comparison.
Important features to note from this pattern are: a 6° beamwidth, an
approximately -21 dB first sidelobe, and sidelobe maxima at 10°, 20°
and 30°.

Disc System I

The parameters of this system were selected with two goals. First,
a null is to be placed at 10°--the maximum of the first sidelobe. The
first sidelobe is the most difficult position to null because it has
the most power. This may also make it the most important position to
be able to null in an actual system. The second consideration was to
make the system as flexible as possible (flexible in terms of being able
to null over a large range of θ).

The second specification makes the optimal position of the preceding
chapter no longer the best. By mounting discs closer to the center of

the aperture than the optimal position, nulling is possible over a larger range of θ. Our main interest is the ability to produce nulls as θ grows larger; no real attempt is made to null into the main beam. The cost of this flexibility, of course, is that a larger disc is required in this position than would be in the optimal position. The performance of this system is shown in Figures 9 through 16.

The fulfillment of the first requirement is shown in Figure 9. By proper adjustment of the two discs, a null is produced at 10°. Figures 10 and 11 show the effects of the discs on the aperture electric field along the x-axis (discs extend from -13 and -6, and 6 to 13 inches). Note the approximate 180° phase shift over the affected area characteristic of a minimum sized disc.

This disc system is capable of producing a null in the radiation pattern anywhere from 7° to 20°. Figure 12 shows a null placed at 20° (the second sidelobe of the undisturbed pattern). Figures 13 and 14 show the discs' effect on the aperture electric field is no longer contained in one zone. (For all sidelobes out to 45° the negative zones are dominant for this antenna system.) Also, the phase shift produced by the discs is much less than 180°.

The extremes of the capabilities of this disc system are shown in Figures 12 and 16. The null shown in Figure 16 at 7° is the "inner limit" of the nulling capability (within a whole degree). Note that this is actually inside the first null of the undisturbed pattern. Figure 12 shows the system adjusted to produce a null at 20°, the "outer limit" of this system's capability.

27

Disc System II

The parameters for this disc system were selected to allow the use of the smallest discs possible to produce a null which was at 31° (The maximum of the third sidelobe). It was desired to have the effective nulling range of this system not overlap with that of system I in order to demonstrate the ability of a set of disc systems to null where neither is totally effective individually.

Disc system II, adjusted to produce a null at 31°, is shown in Figure 17. The modulated electric fields in this configuration are shown in Figures 18 and 19. Again, note the approximate 180° phase shift over the area affected by the disc.

This system is capable of generating nulls from 24° to in excess of 60° which is the outer range where this model is considered valid. The radiation pattern of the antenna with the disc system adjusted to produce a null at 24° is shown in Figure 20.

A null in the radiation pattern at 45° is shown in Figure 21. This pattern is of interest for two reasons. Examining Figures 22 and 23, the modulated electric fields along the x-axis for this configuration reveal the narrow width of the zones at this angle (one quarter wavelength).

A second interesting property of this nulling method becomes evident comparing Figures 17 and 21. In Figure 17 the desired null is at 31° and the pattern at 45° is approximately at the same level as the undisturbed pattern. Figure 21 shows the desired null at 45°, but also shows the pattern level at 31° is over 40 dB down from the undisturbed pattern. Thus, Figures 17 and 21 demonstrate that one disc system may be able to provide a reasonable amount of cancellation to more than one noise

28

source if both sources were considered at the same time. (This was not
feasible using the simple code in the appendix; however, in an actual
system the algorithm would likely have to respond to total noise power
because no distinction would be available between noise from different
angles.)

Disc System III

What is now defined as disc system III is actually the combination
of systems I and II. As noted earlier, these two systems do not overlap,
and thus could be mounted on the same dish. The problem we wish to address
is whether the two systems together can accomplish what neither can indepen-
dently, i.e., provide a nulling capability between 20° and 24°. Figure 25,
with a null at 22°, demonstrates that this is indeed possible; the effects
of the two systems may be seen to add directly. This would be expected
since the discs simply act to reduce the magnitude of the P-component.
This effect adds in a linear fashion; however, since the pattern strength
is proportional to the magnitude of the P-component squared, the amount
of cancellation available is much greater than a linear sum. This model
shows both disc systems must be able to provide some cancellation; if
a system is not able to provide any cancellation, adding it to another
system simply degrades the performance of the effective system.
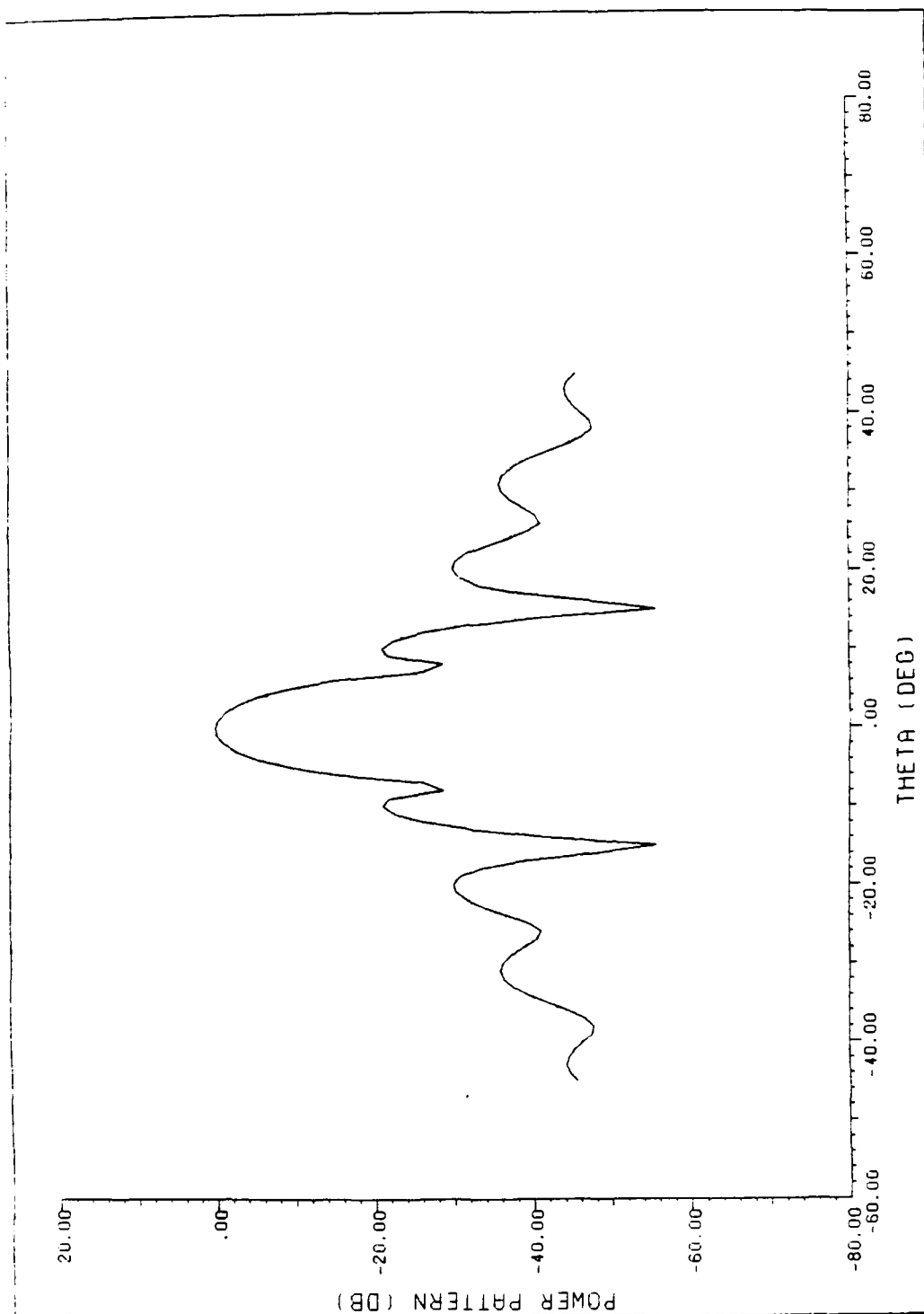
Figure 8. Unmodified H-Plane Radiation Pattern of Four-Foot Aperture

30
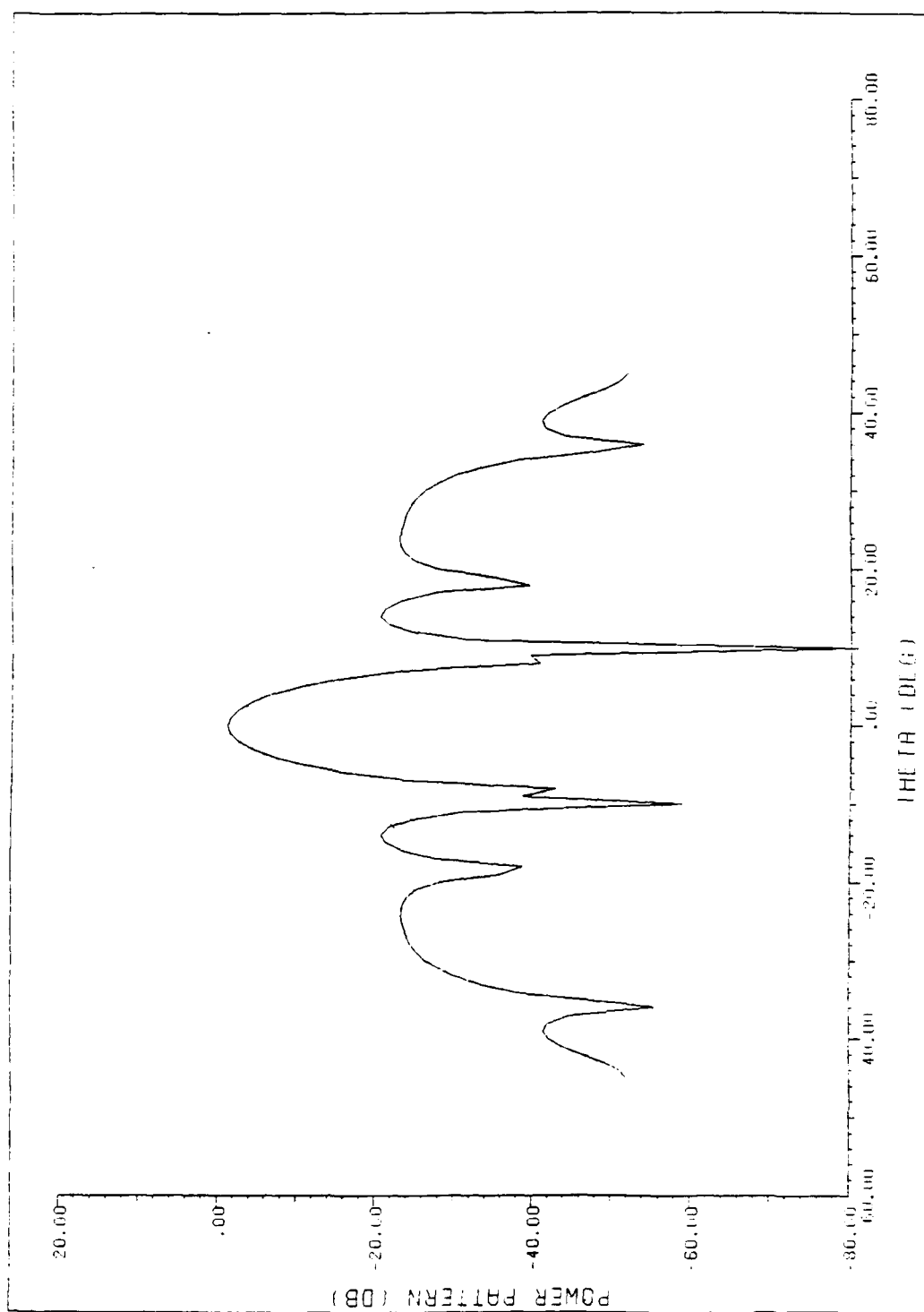
Figure 9.   H-Plane Radiation Pattern With Null at θ=10°
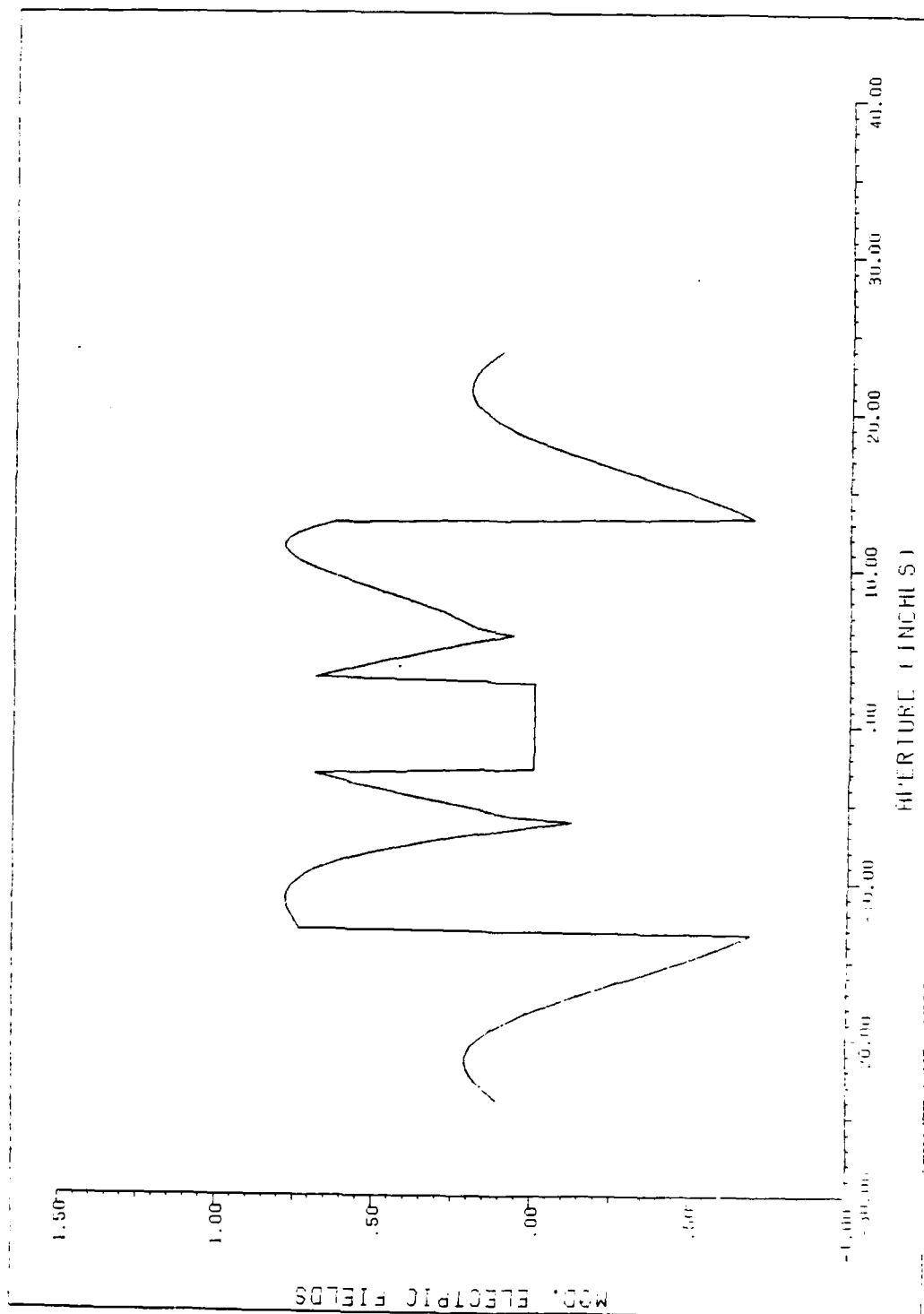
Figure 10. Cosine Modulation on x-Axis With Null at θ=10° (Disc System I)

32
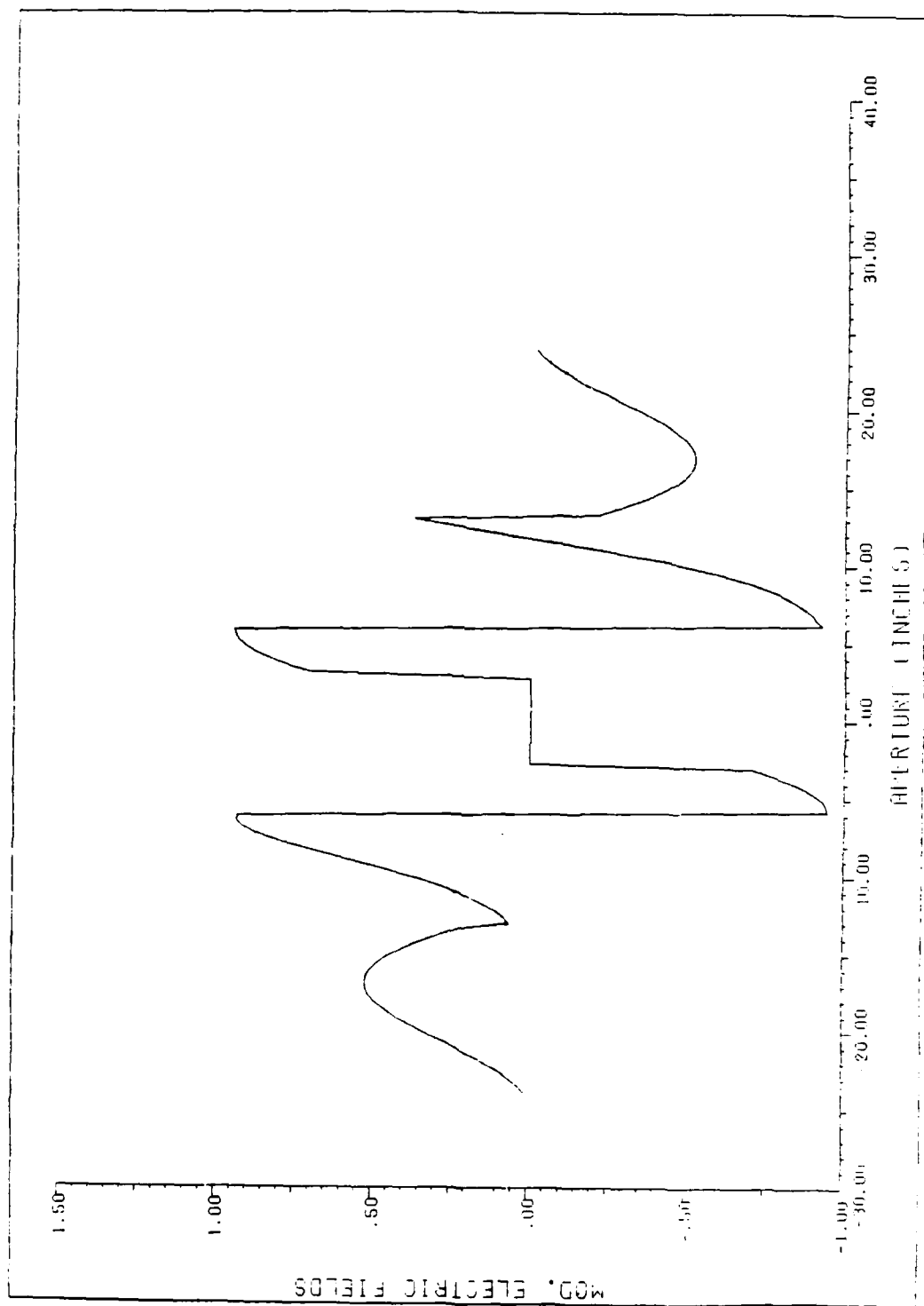
Figure 11.   Sine Modulation on x-Axis With Null at θ=10° (Disc System I)
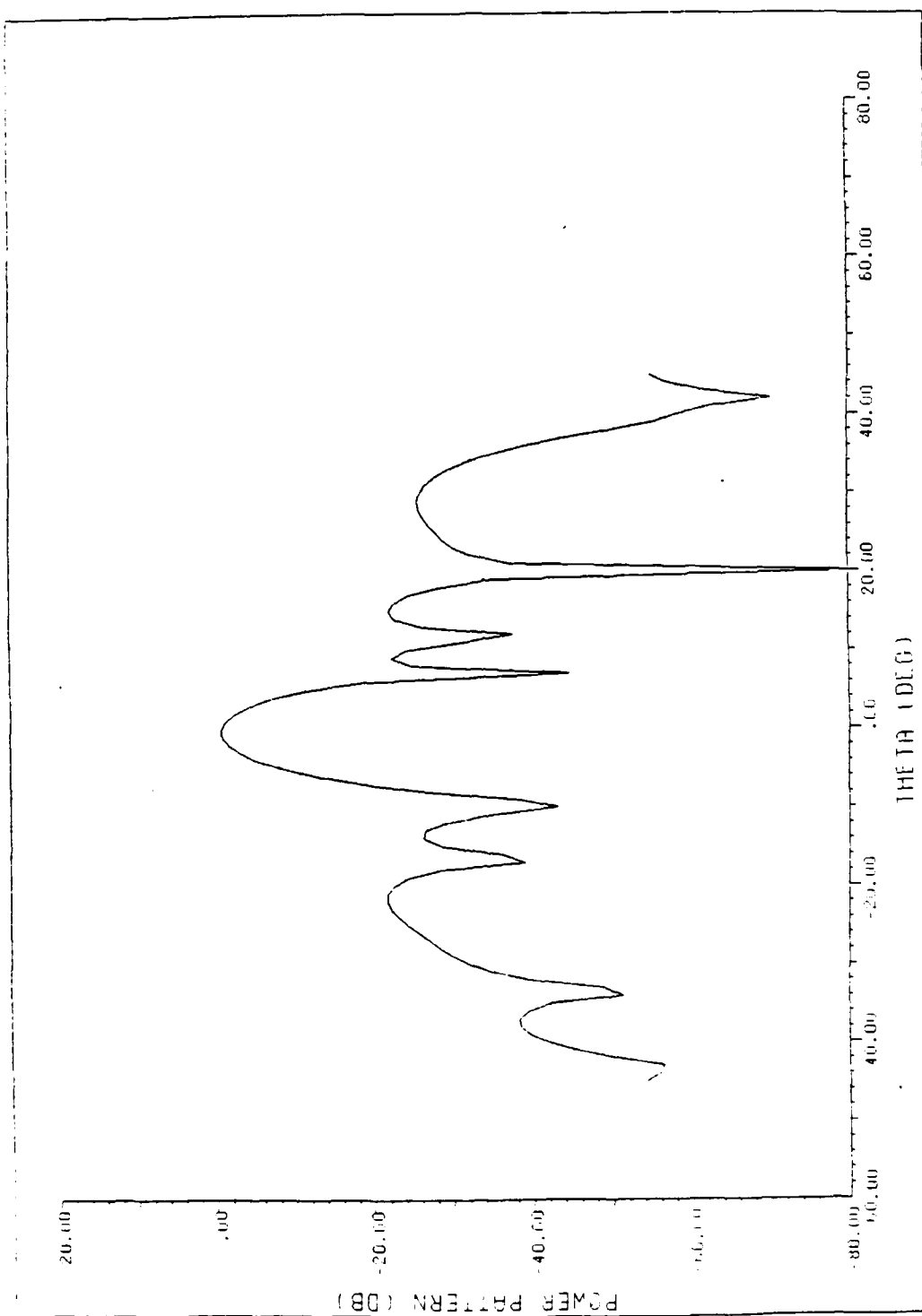
Figure 12.   H-Plane Radiation Pattern With Null at ⌐=20° (Disc System I)

MOD. ELECTRIC FIELD

APERTURE (INCHES)
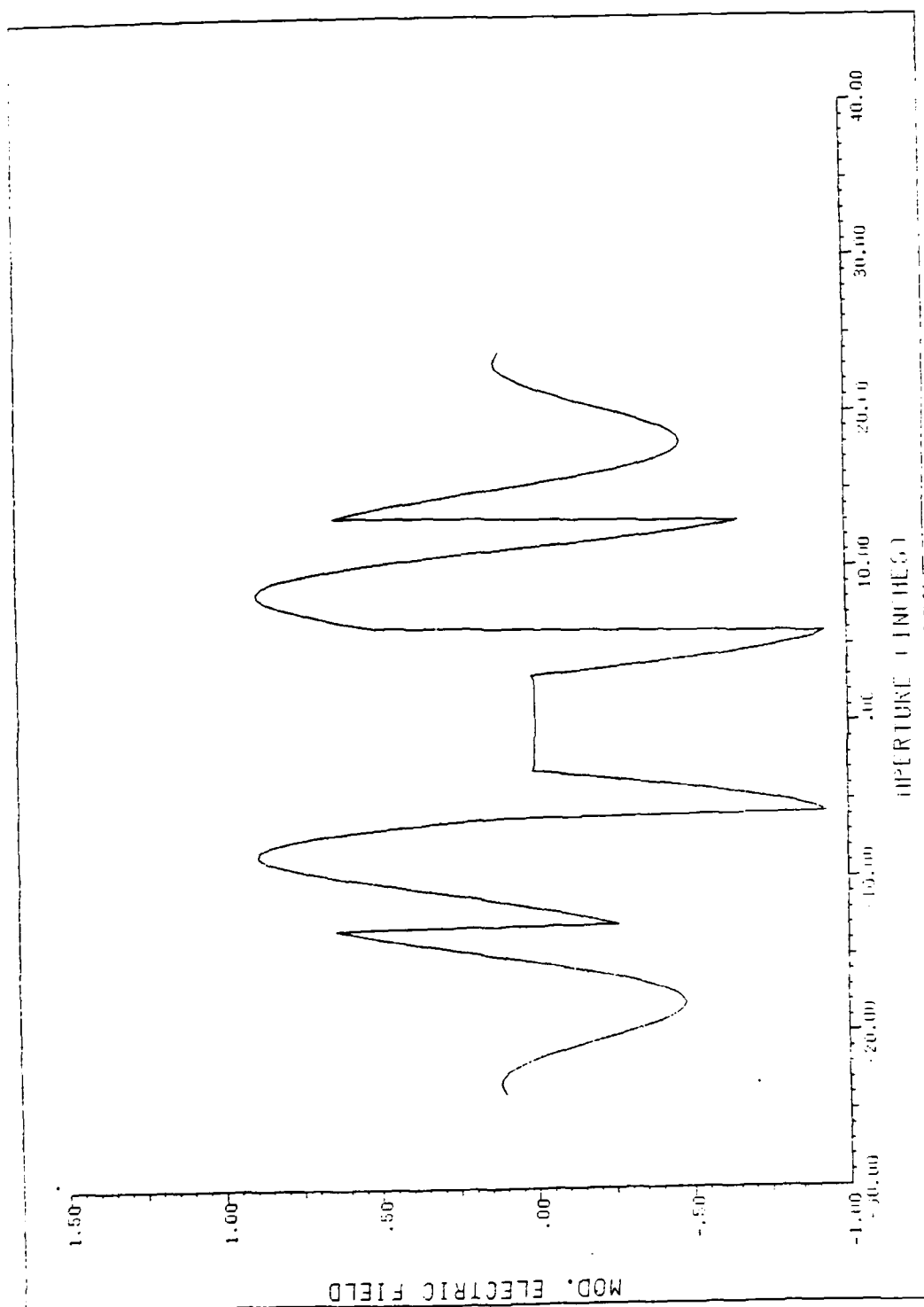
Figure 13.   Cosine Modulation on x-Axis With Null at θ=20° (Disc System I)

35
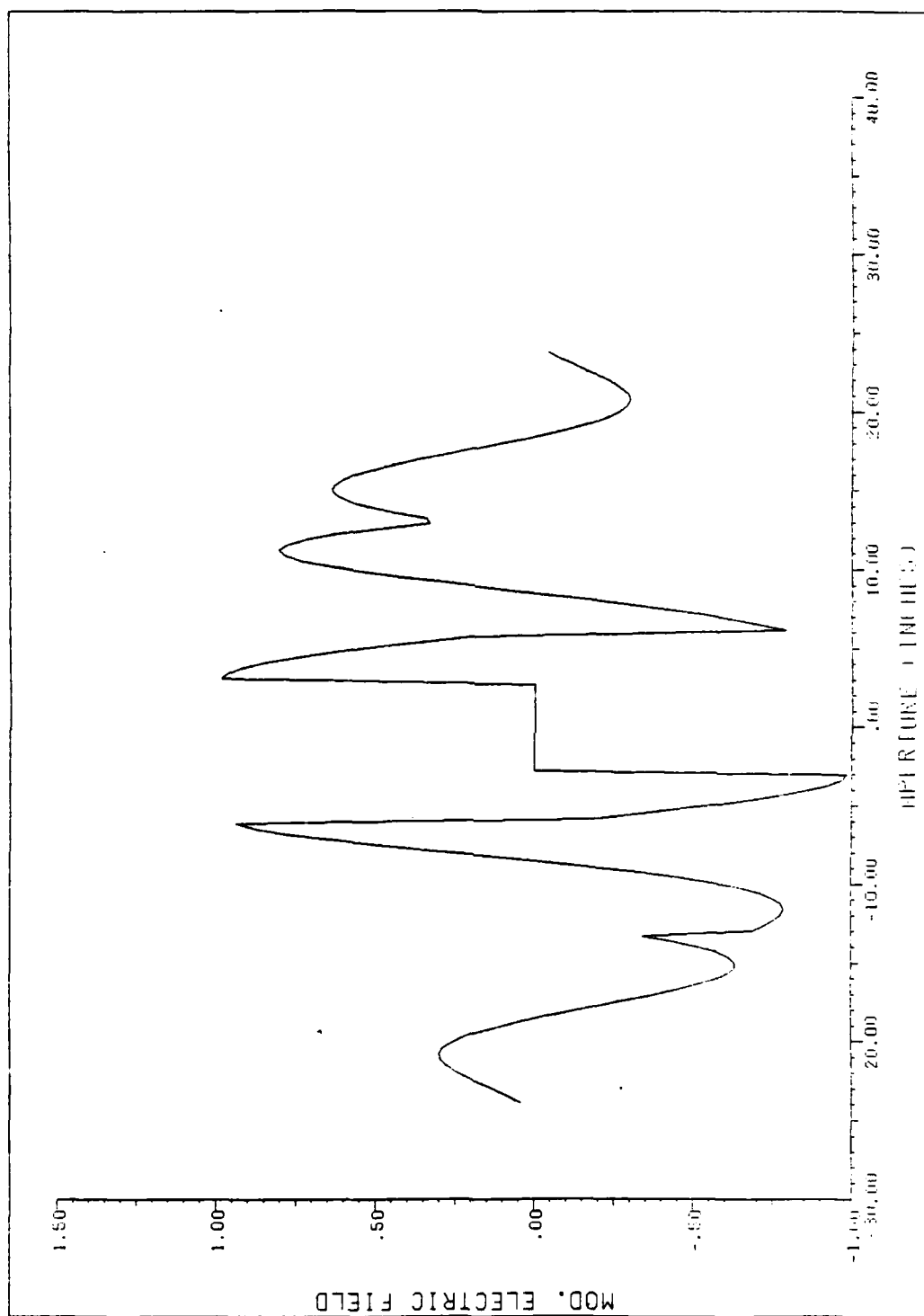
Figure 14.   Sine Modulation on x-Axis With Null at θ=20° (Disc System I)

36
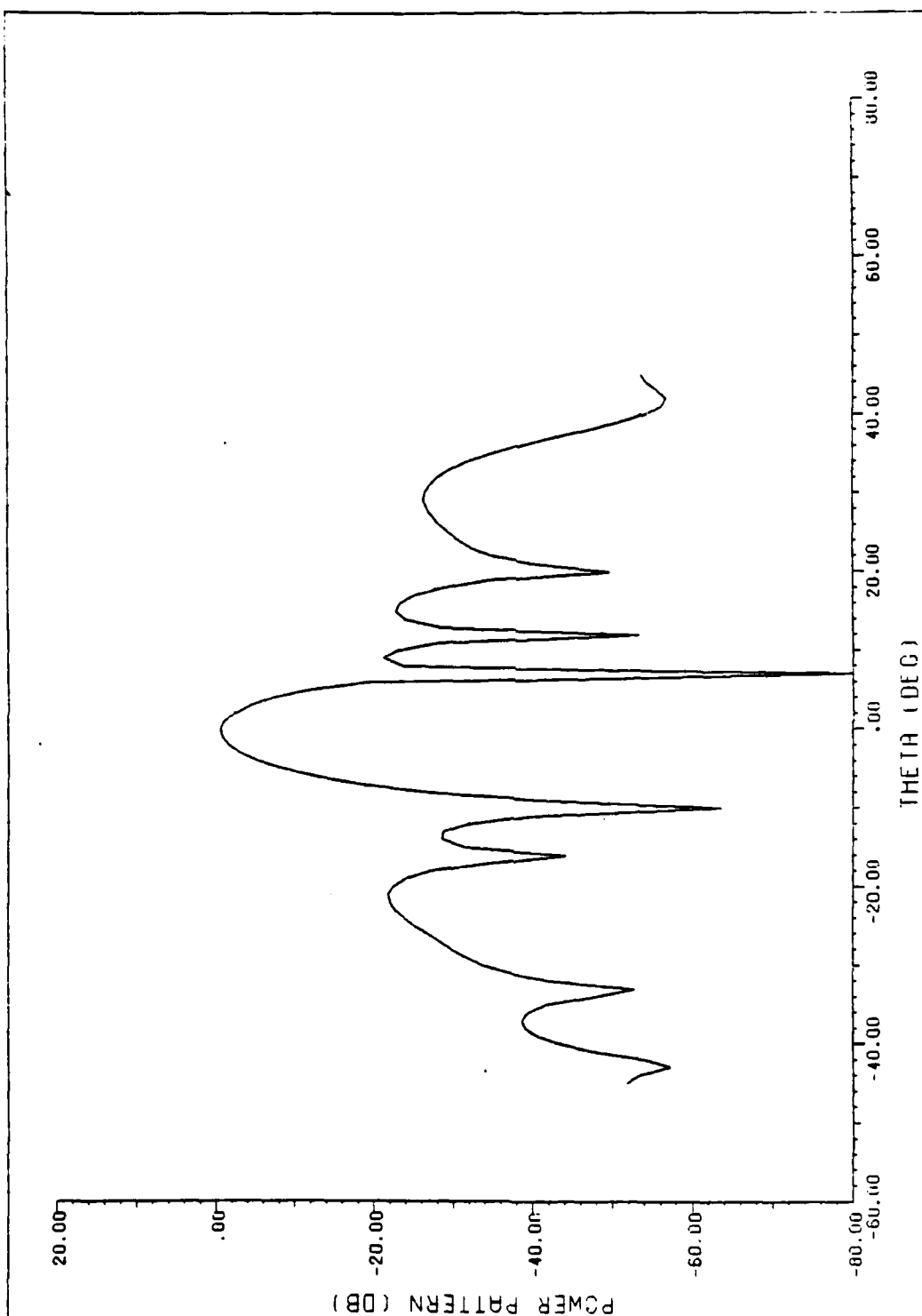
Figure 15. H-Plane Radiation Pattern With Null at θ=7° (Disc System I)

37
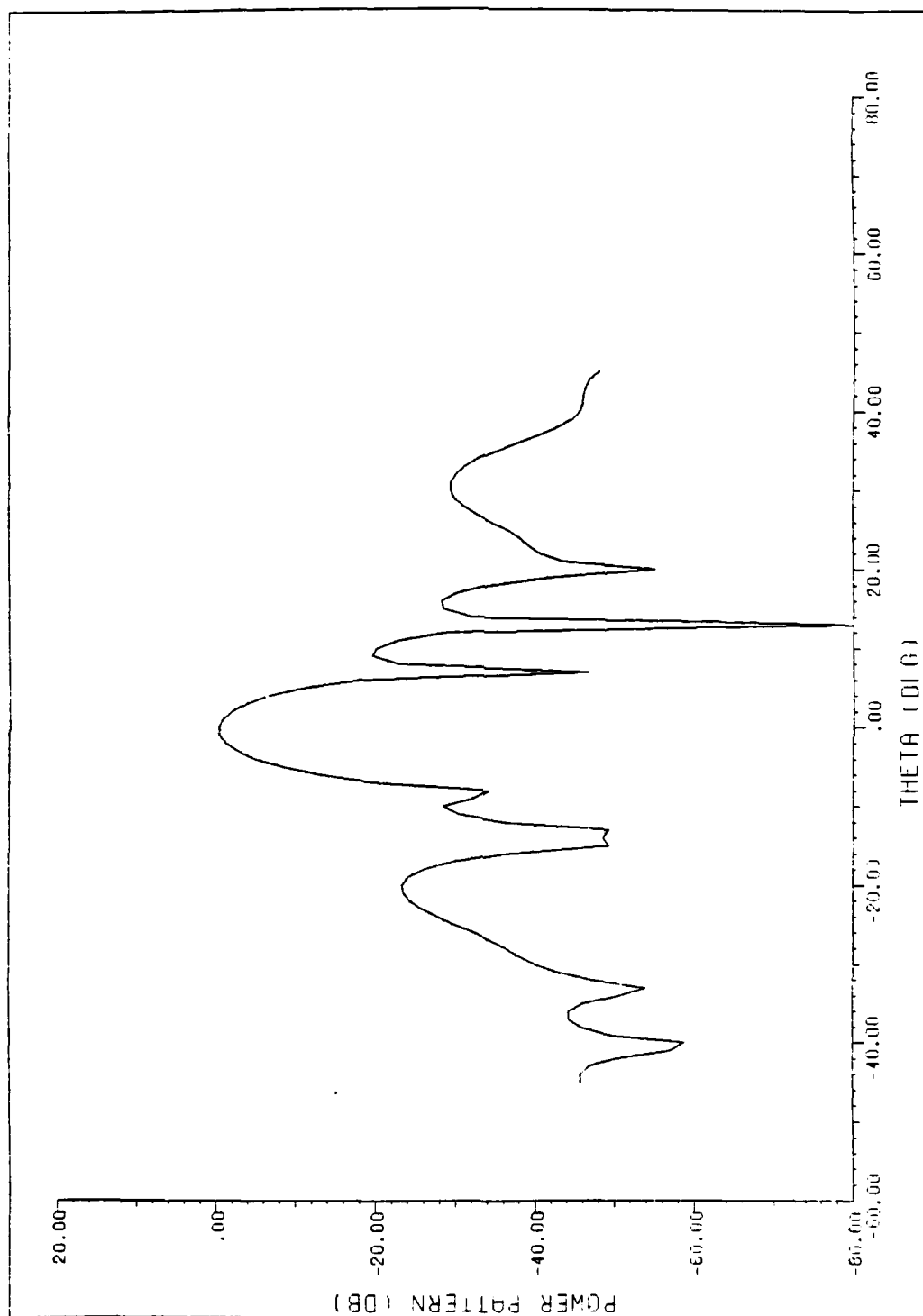
Figure 16. H-Plane Radiation Pattern With Null at θ=13° (Disc System I)

38
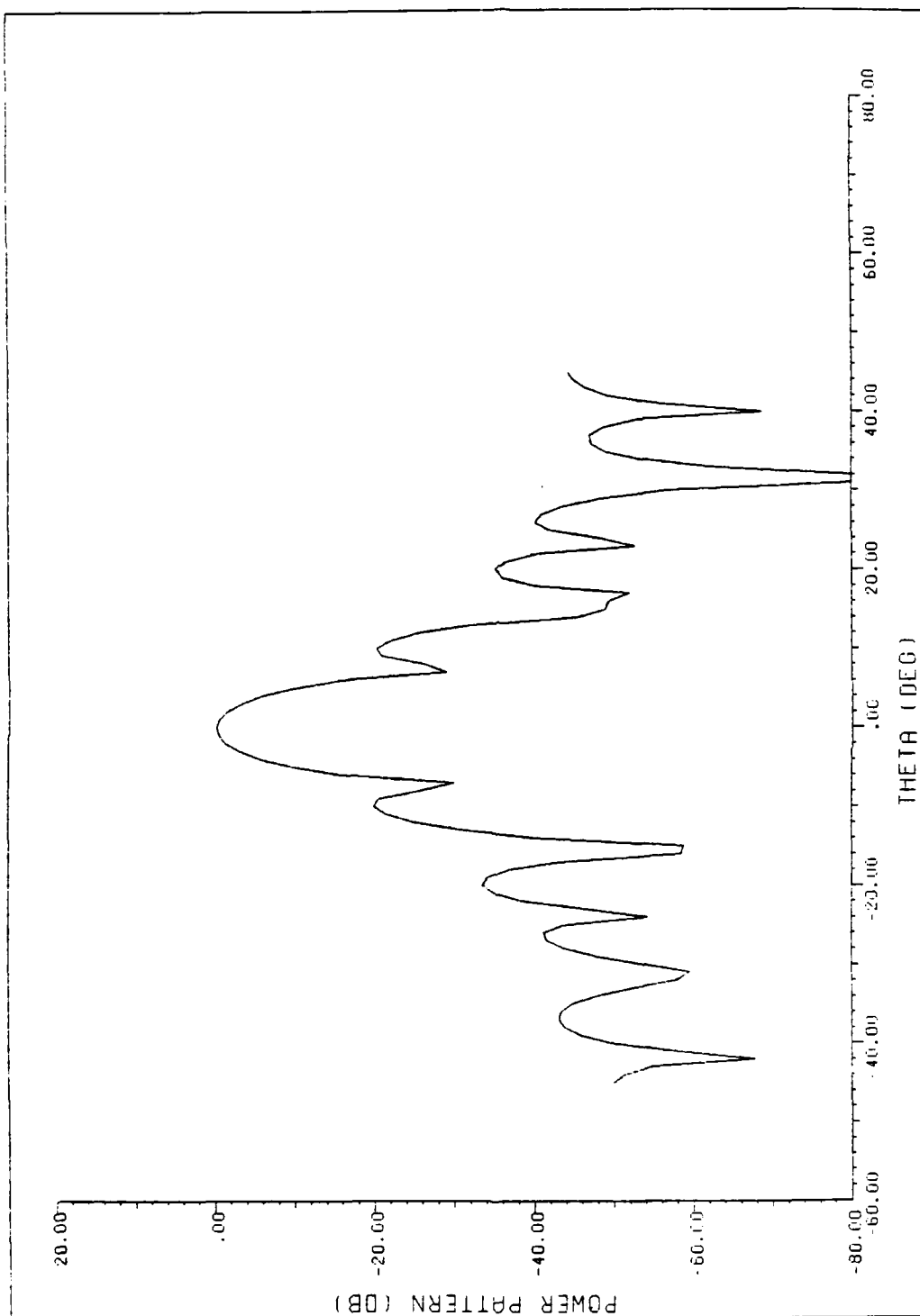
Figure 17. H-Plane Radiation Pattern With Null at θ=31° (Disc System II)
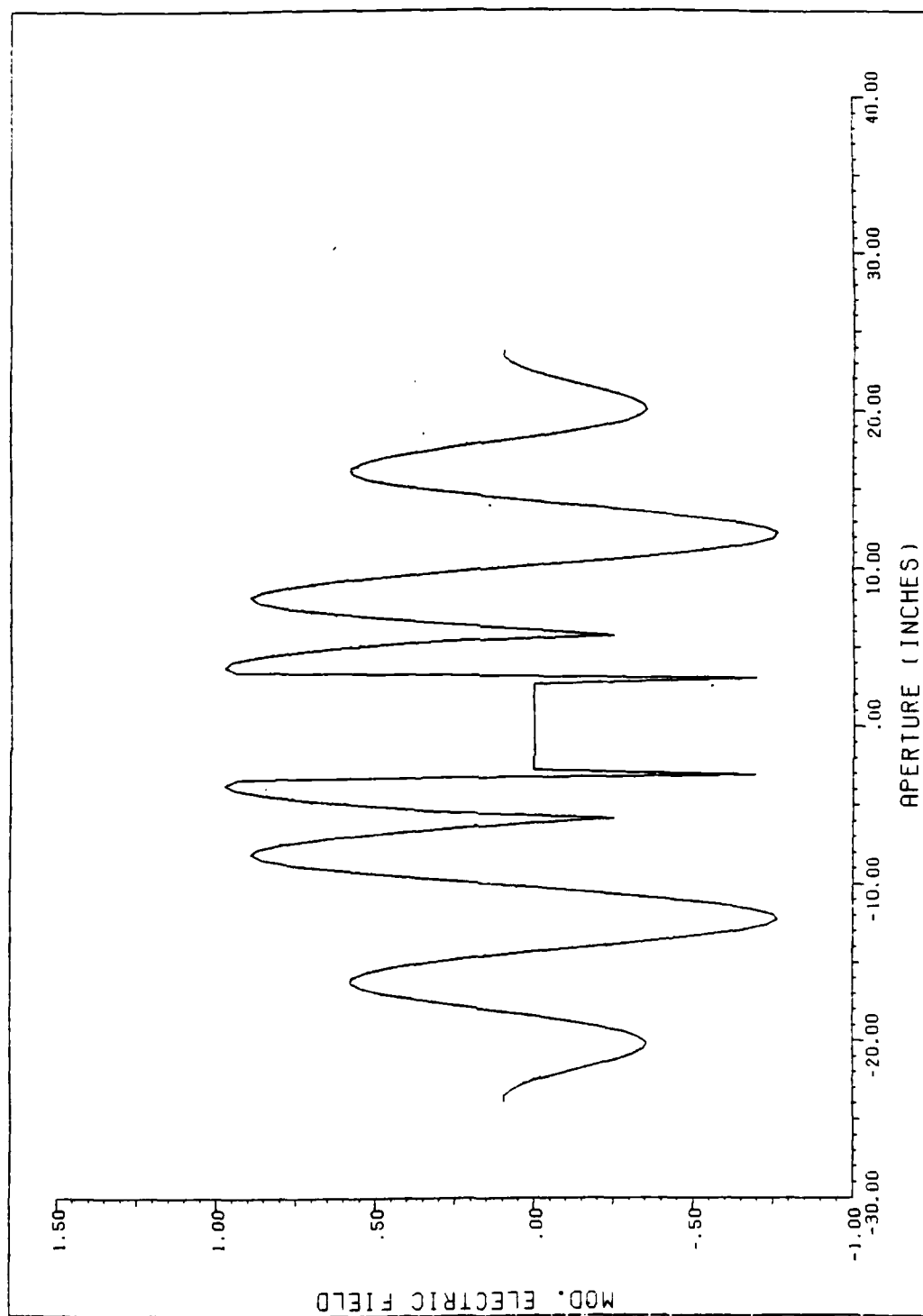
Figure 18. Cosine Modulation on x-Axis With Null at θ=31° (Disc System II)
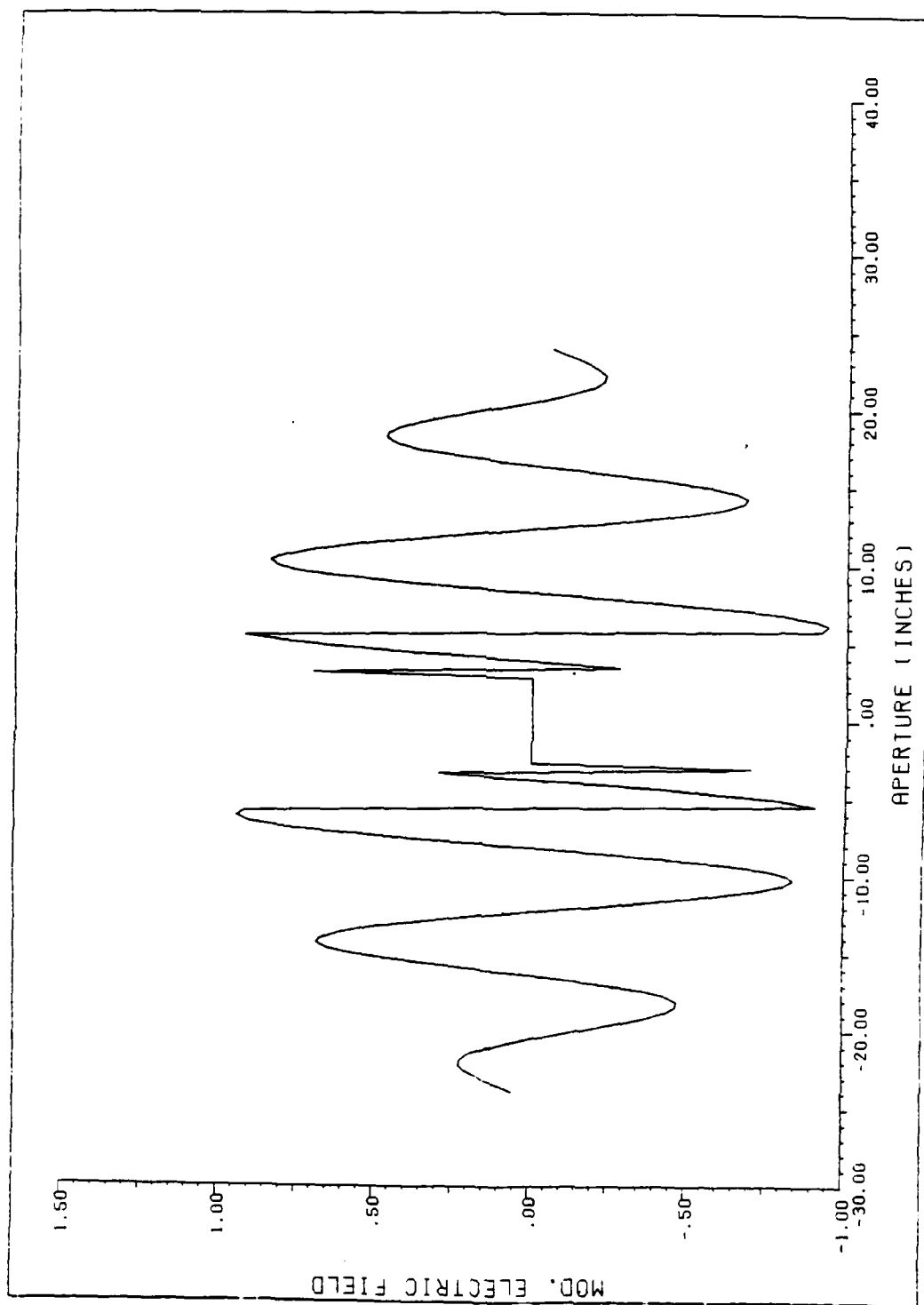
Figure 19. Sine Modulation on x-Axis with Null at θ=31° (Disc System II)

41
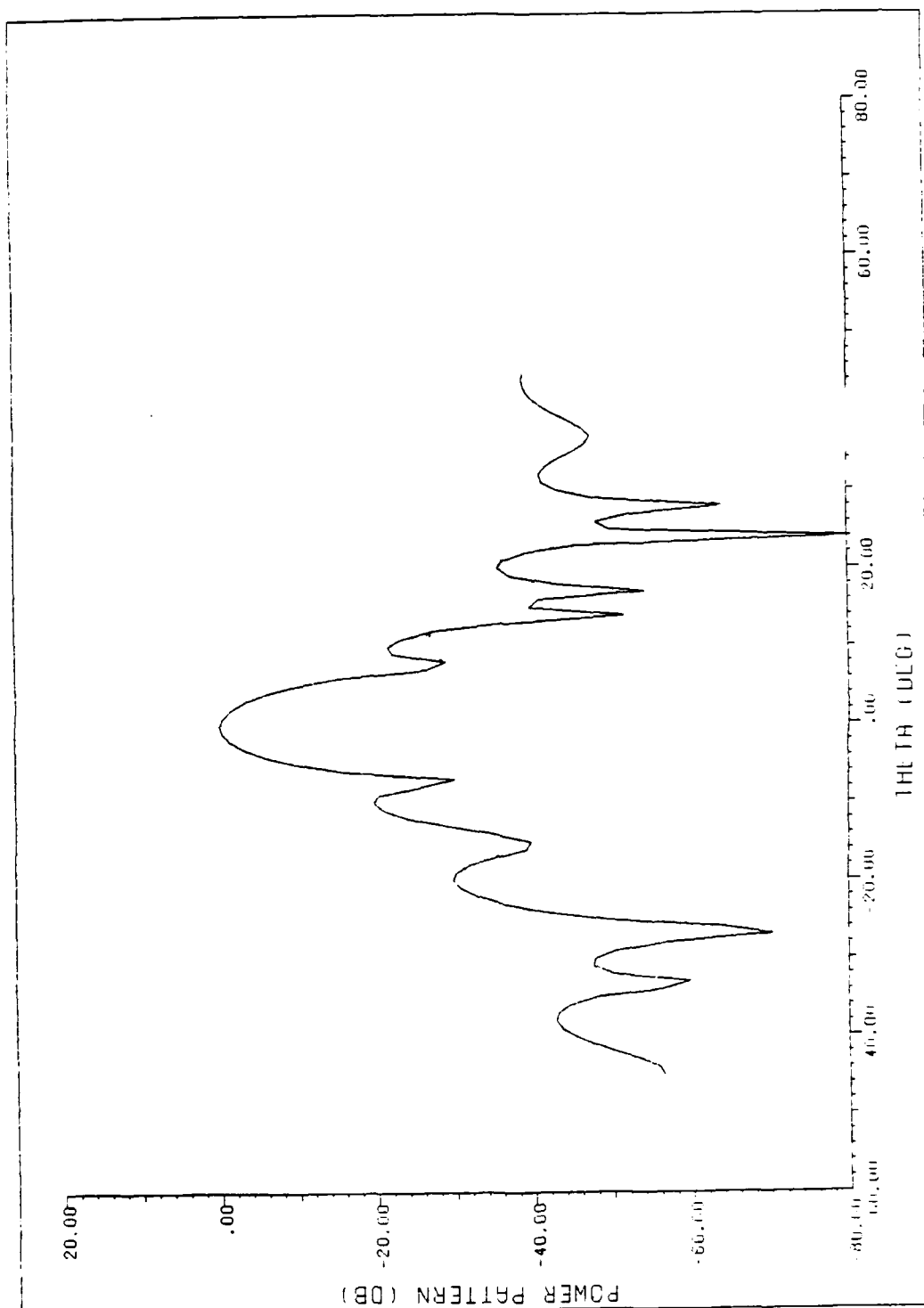
Figure 20.   H-Plane Radiation Pattern With Null at θ=24° (Disc System II)

42
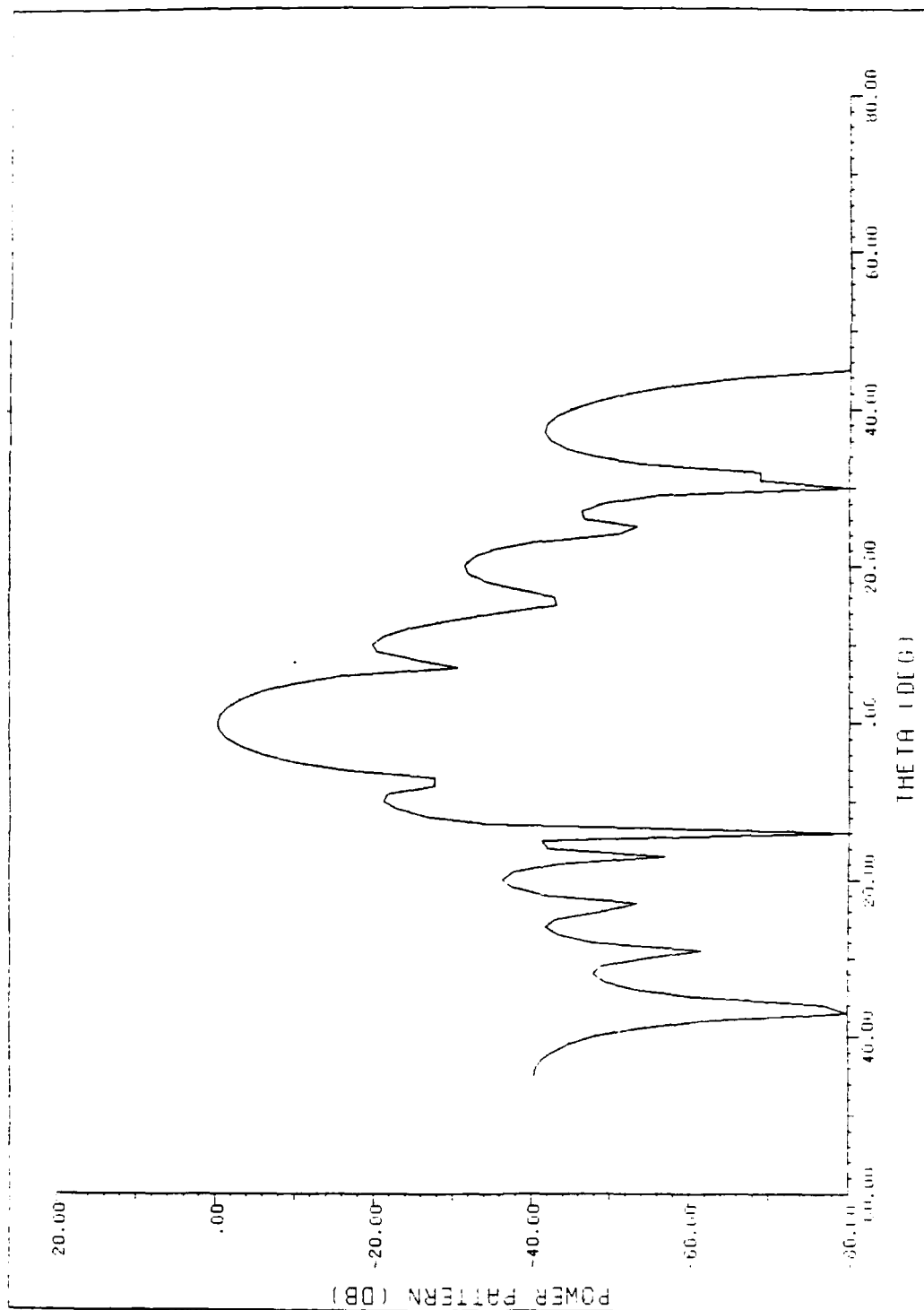
Figure 21.   H-Plane Radiation Pattern With Null at θ=45° (Disc System II)

43

Figure 22. Cosine Modulation on x-Axis With Null at θ=45° (Disc System II)

44

Figure 23. Sine Modulation on x-Axis With Null at $\theta=45°$ (Disc System II)
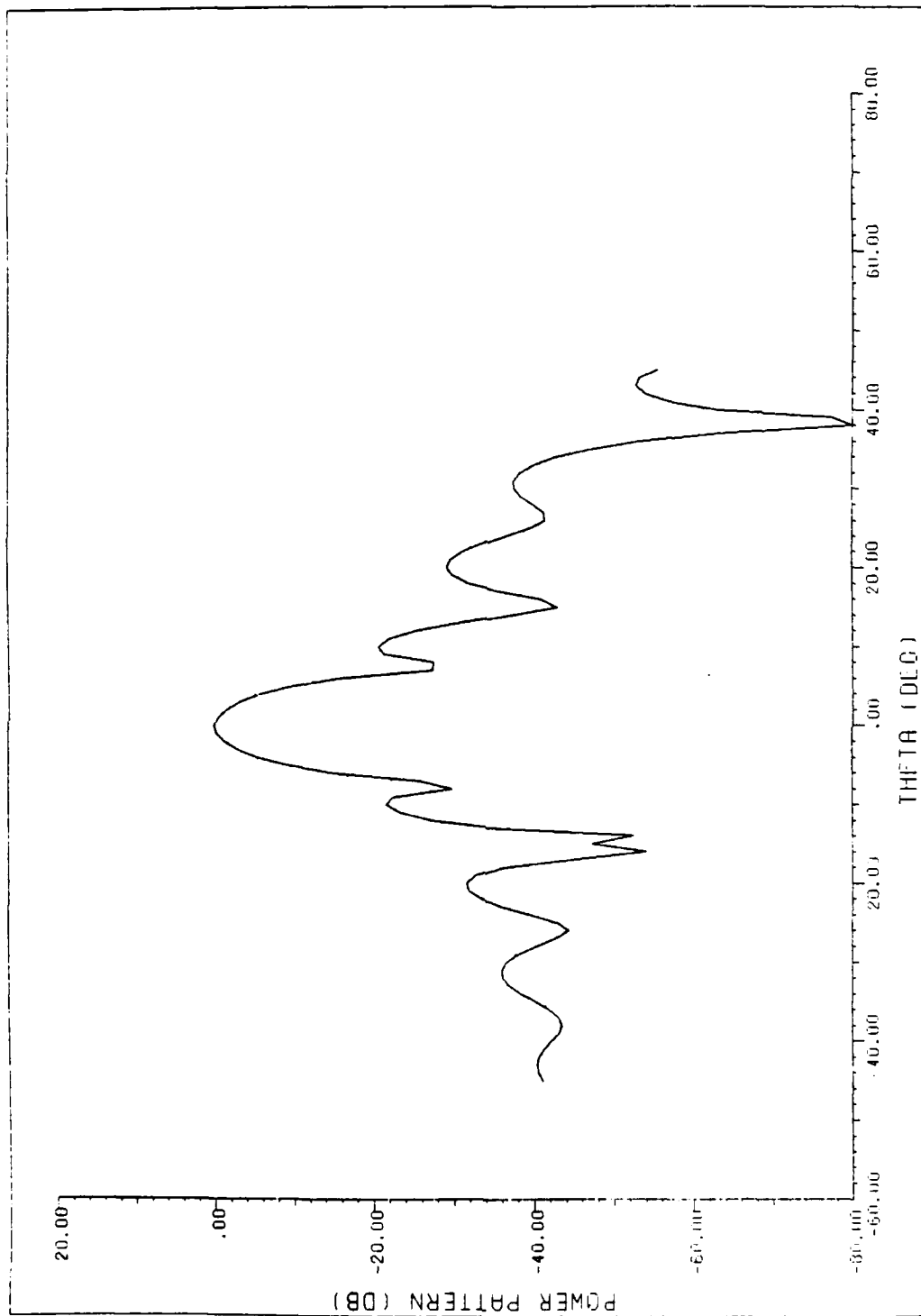
Figure 24.   H-Plane Radiation Pattern With Null at θ=38° (Disc System II)
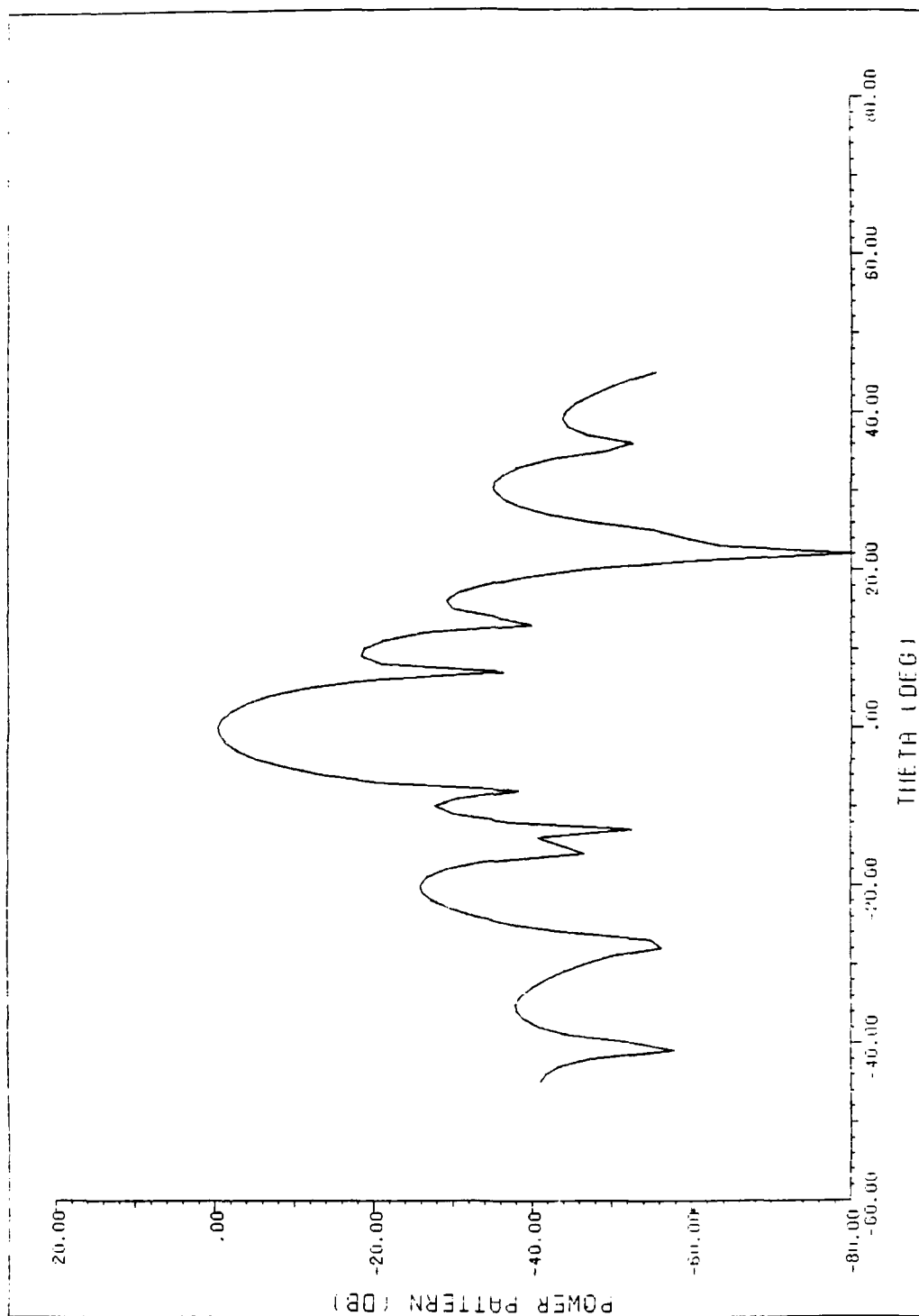
Figure 25. H-Plane Radiation Pattern With Null at θ=22° (Disc System III)

System Bandwidth

The other effect investigated using this model was the effect of frequency on the antenna pattern containing nulls. Since most noise sources contain more than a single frequency (except perhaps a tone jammer), the width of a null in frequency has a definite bearing on system capability in any realistic situation. The feed (or receiver) in an actual system may provide noise rejection outside the design bandwidth. However, most systems must be designed to operate over some finite bandwidth and are susceptible to noise in this bandwidth.

Frequency Performance Plots

The disc systems used to generate these plots are the same as used in the previous sections. Referring to Figures 26 through 29, actual pattern points were calculated only at the frequencies shown as asterisks on the "without discs plot." Thus, the data is actually only exact at the thirteen frequencies with a straight line connecting these points to show an estimate of performance.

A point to consider analyzing these plots is that while performance is examined over a 20% bandwidth, the discs were adjusted to provide cancellation at the center frequency. The code used has no provision for cancellation over a finite bandwidth. An actual system, however, could be designed to do so. While no claim is made that the discs could be adjusted to provide a -80 dB null over a finite bandwidth, a better adjustment than shown may be possible (in terms of minimizing total noise power to the receiver) if the adjustment were done with respect to the entire bandwidth.

48

Figure 26. This plot shows the performance at 7° with disc system I adjusted in the same manner as Figure 16. This demonstrates the problem with locating a null in close proximity to a null in the undisturbed pattern (pattern of the antenna without discs). The change in frequency has effectively moved the first null in Figure 8 "in" to 7° at 3.0 GHz. Thus the disc system provides cancellation performance only at frequencies less than approximately 2.9 GHz.

Figure 27. This is the performance of the same antenna and disc as shown in Figure 10 at 10°. While performance is obviously best at the center frequency, there is cancellation over approximately a 10% bandwidth. As discussed before, it may be possible, with different disc adjustment, to provide better cancellation over the entire bandwidth by sacraficing some cancellation at the center frequency.

Figure 28. This is disc system II's performance at 20° with the same adjustment as Figure 13. This shows good performance over almost a 20% bandwidth with especially good performance over the lower half of the frequency range.

Figure 29. This figure shows the performance of disc system II with the same disc settings as Figure 18 at 31°. Again, excellent performance is noted over a 10% bandwidth with cancellation available over almost all of the 20% bandwidth.
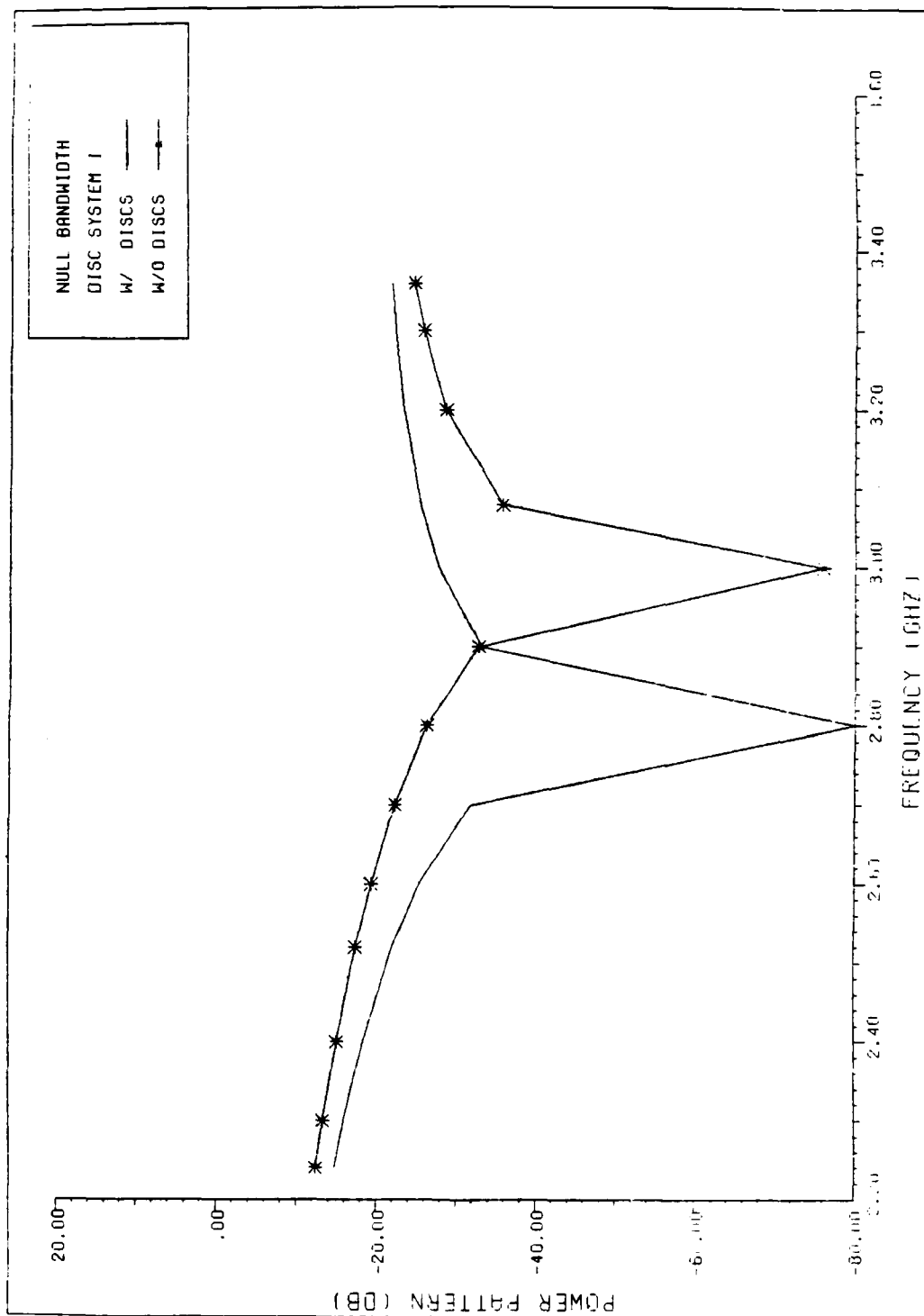
Figure 26. Frequency Performance of Disc System I With Null at θ=7°
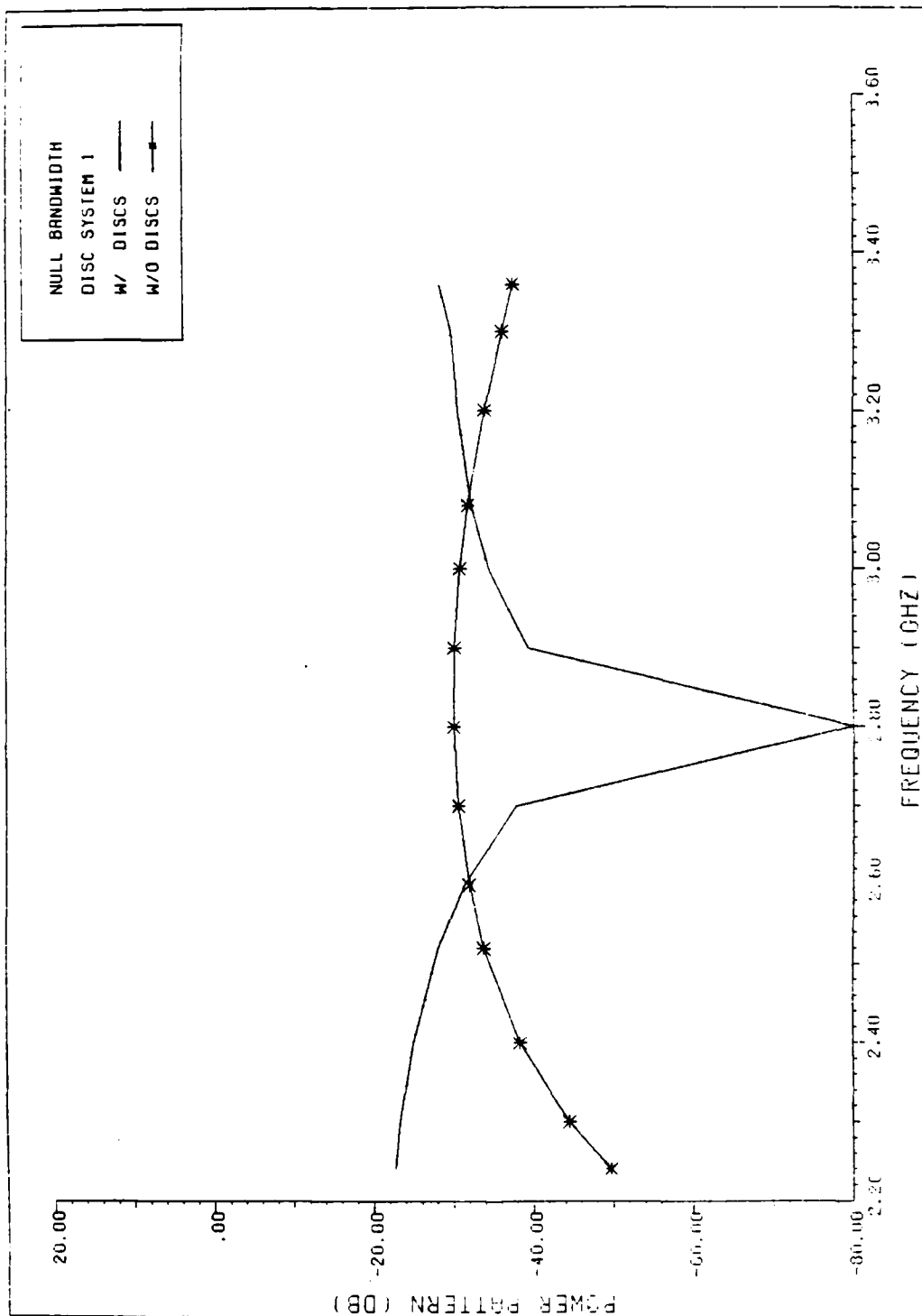
Figure 27. Frequency Performance of Disc System I With Null at θ=10°
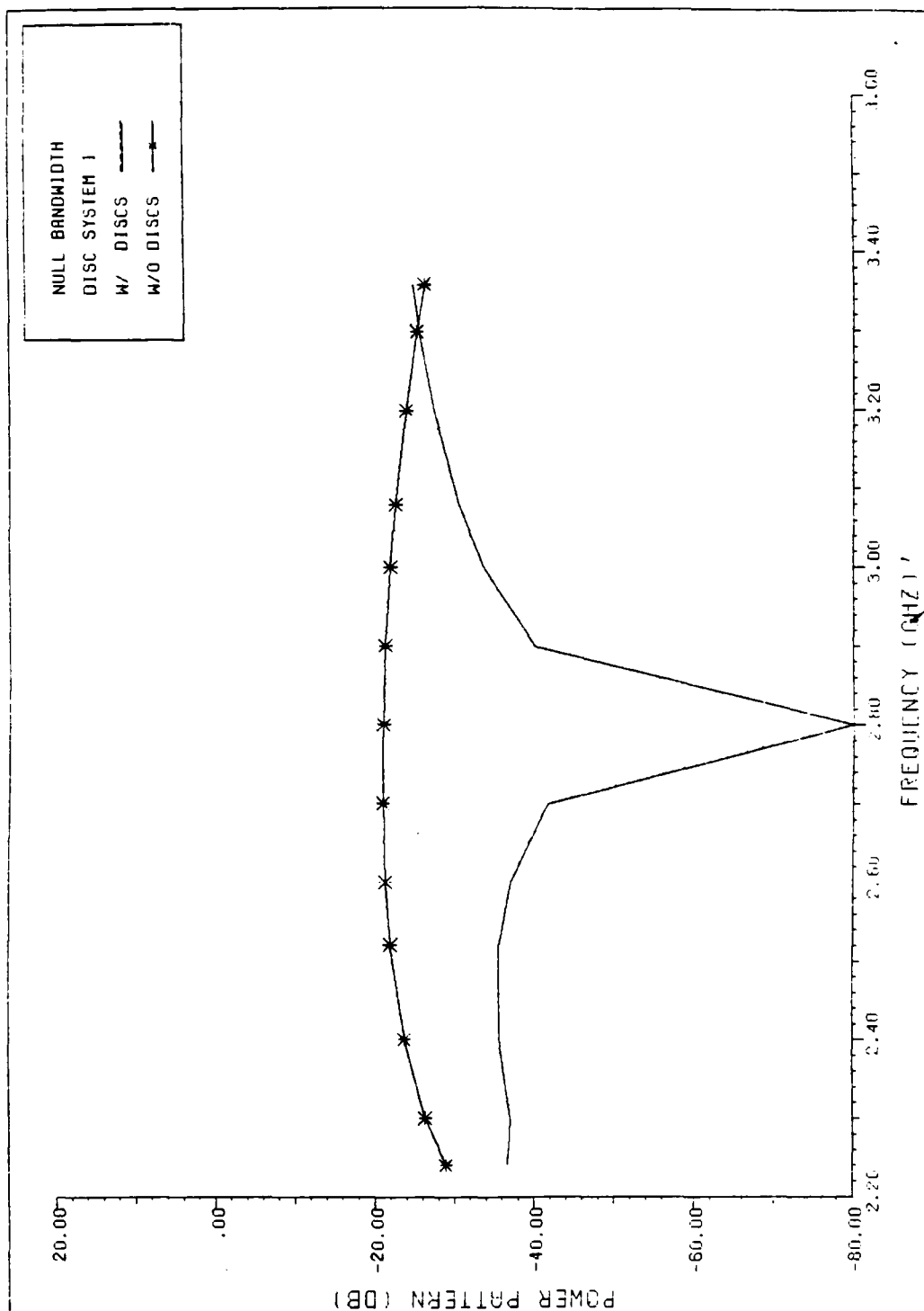
Figure 28.   Frequency Performance of Disc System I With Null at θ=20°
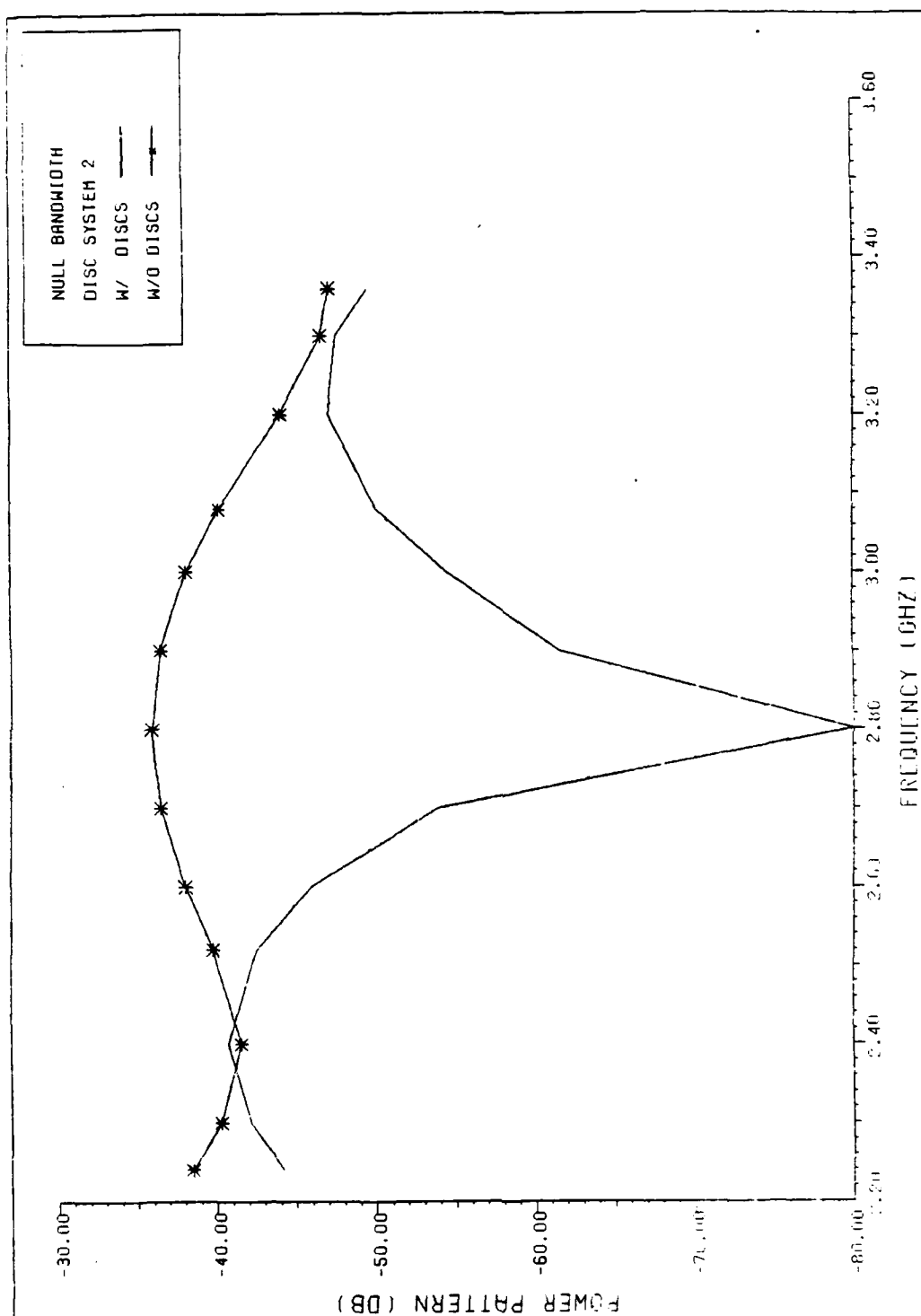
Figure 29. Frequency Performance of Disc System II With Null at $\theta = 31°$

Conclusion

The theoretical model presented, while not producing any exact
equations for the disc system, does offer several "rules of thumb." Any
exact formulation would have to be suspect regardless, since this is
only a first order model. Even assuming an ideal feed and perfect
reflector, second order effects, such as diffraction, become significant
in the sidelobe region.

Disc Effects

The discs were found capable of generating the desired nulls in
the radiation pattern while leaving the main beam gain relatively unaffected.
The maximum gain loss is only slightly over one dB (1.2 dB on the pattern
with a null at 10°).

The three dB beamwidth was affected even less, although as pattern
levels were calculated only every degree, exact numbers are not available.
The discs do cause sidelobe levels to be raised; however, no sidelobe
was raised above -20 dB (only 1 dB higher than the undisturbed first
sidelobe level). Overall performance is excellent, and in general agree-
ment with performance as demonstrated experimentally by Jacavanco
(Jacavanco, 1984a).

Dish Size

It should be noted that all work done (both experimentally by Jacavanco
and in this model) has been with reflectors that are relatively small
in terms of wavelengths. A problem is that while the zone widths are
independent of the reflector size (see Eq (14)), required disc size is
not (see Eq (16)). Simply enlarging the disc in direct proportion to

54

the reflector therefore will not give equivalent performance with a larger reflector. Because the larger disc will span more zones, its effective area will be smaller. One solution would be to use an increased number of smaller discs on the larger reflector (appropriately placed in the zones). Another option would be to use a shape other than the circular disc to supply an equivalent area in the zone.

Comparison of Model with Experimental Results

In order to try and validate this model, experimental data was obtained from Daniel Jacavanco (Jacavanco, 1984b). All attempts to recreate or match these results failed. This failure is thought to be a result of poor data on the antenna used in the experiment, not a failure of the basic theory.

Two basic characteristics of the antenna used in the experiment were not well-known when the attempt to match results was made. The first is the actual aperture distribution produced by the feed. The distribution was modeled as a parabolic taper of order one on a 20 dB pedestal. Data obtained on the radiation pattern of the feed subsequently has shown that although the pedestal height was approximately correct, the taper estimate was too steep.

The second error in the antenna as modeled was the assumption that the reflector was a perfect paraboloid. The actual antenna used in the experiment was a general purpose, medium performance reflector. When the surface of the reflector was measured it was found to have significant errors. This is characteristic of medium performance reflectors, but is difficult to model.

Either of these errors in the model could cause failure of the model to match experimental results. It is not surprising, then, that no correlation could be found between the experimental and model results. Another attempt is being made to correct the model and match results. This should be the primary goal of any further research.

Areas of Further Investigation

There are several areas where more investigation on this topic may provide valuable results. As mentioned earlier, however, any further research should probably begin with an attempt to develop a more accurate model of the antenna used in the work by Jacavanco, in order to match experimental results. This is not a trivial goal as errors in the reflector surface will be difficult to accurately model. To establish confidence in this approach, however, corroboration by experimental results is essential.

Rectangular Sections

The zones produced by this approach suggest another method of implementing this basic idea. Rectangular sections, instead of discs, mounted with their long axis perpendicular to the axis of the desired null would appear to be a more efficient system. This system could be adjusted either by varying the sections' distance off the reflector in the same manner as the discs, or by mounting them one-fourth wavelength off the reflector (to produce a 180° phase shift) and moving them laterally to adjust the pattern. Either system would be a more complicated mechanical arrangement than the discs, but performance gains may be worth the complexity.

Polarization dependence is a problem that an analysis of this system would have to consider. If the sections were mounted such that their long axis was not collinear with the feed polarization, their effective area would likely be reduced. An approach other than geometrical optics would have to be employed, and this limitation considered, in any comparison of performance.

Adaptive Array

Another area of interest would be the design of an array of discs mounted on a dish to provide nulling at an arbitrary angle. An algorithm to control the discs to provide an adaptive system could then be considered. Main beam gain would suffer excessively if too many discs were mounted on the dish. However, a system that used discs made of metalized plastic that could be pulled back flush to the dish when not in use might overcome this problem. An algorithm that could efficiently control such an array would be a challenging project. If such a system could be shown to be feasible, it could provide an attractive alternative to a conventional adaptive array in some applications.

Number of Discs Required Per Null

The array problem brings to light another question that, while theoretical, is of practical interest. The model as presented in this paper demonstrates that the generation of a single null requires two discs. Daniel Jacavanco has proposed that in general to generate n nulls in the far field pattern would require, following from array theory, n+1 discs (Jacavanco, 1984a). The theory of this paper, however, would seem to suggest that two discs per null may be required, as for each

57

null you must control two variables (the imaginary and real parts of
the P-component). Because these variables are not independent, however,
it is not immediately clear whether two discs are required or not. An
investigation of the number of discs required to produce n nulls at arbitrary
locations would definately be of interest to any future research on arrays
of discs.

Optimum Distortion

The discs are a method of reflector distortion that, while easily
fabricated and adjusted, do not offer an optimum solution. Eqs (10)
and (11) do, however, offer a solution for an optimal distortion. If
the distortion induced was such that the argument of the sinusoids was
equal to an even or odd integer multiple of pi (depending upon which
zone was dominant), the maximum cancellation per area distorted would
be realized. Note that two mirror image areas, symmetrically placed
across the aperture, would still be required to insure a zero contribution
from the imaginary part of the P-component. Note also a perfect surface
over the rest of the reflector is required to insure optimal null
generation.

A scheme of this sort, while optimal (in terms of minimum area
distorted per cancellation), may not be preferred in an actual implemen-
tation. One of the main problems with this solution is that it would
require the exact desired null position to be known. While it is relatively
easy to imagine an array of discs controlled by some algorithm to provide
a degree of adaptive nulling, no simple method is readily apparent to
adaptively implement this scheme.

58

Another problem that this system would appear to have is that since the solution is optimal, it would be much more sensitive to variations in either angles or frequency. Sensitivity to the noise sources' movement in the far field may or may not be a problem depending on scenario. However, a high sensitivity to frequency (i.e., a narrow bandwidth null) would cause problems in almost any imaginable implementation.

Summary

The initial objective was to develop a model that would explain the nulling performance of discs mounted on a reflector as demonstrated by Jacavanco (Jacavanco, 1984a). Aperture integration was selected as a well-known technique that appears well-suited to the analysis of this antenna system. While the model developed is only a first order approximation, the important aspects of the system appear to be accurately represented.

The model developed is broken down mathematically to provide insight into the mechanism of null generation and its control. Guidelines are developed for disc placement for null generation based on this model. No satisfactory guidelines were found for required disc size although a rough method of estimation is presented.

The mathematical model is implemented in Fortran code and is exercised to demonstrate its ability to generate nulls. The computer model exhibits the properties predicted by the basic theory and is used to further examine system characteristics such as bandwidth performance. Theoretical results from the model were compared to experimental results without success. This is thought to be a result of too idealistic an antenna model rather than error in the basic theory.

59

Appendix

Computer Codes

Listed are the codes used in the computer analysis of this work.
The codes are a straightforward implementation of the equations of
Chapter One. Both are written in standard Fortran 77.

Method

The aperture is partitioned into hexagons, and the hexagon sampled
at 7 points to approximate the double integral (see Abramowitz and Stegun,
1972:894). The variables PXR, PXI, PYR, and PYI are the variables of
summation for the real and imaginary part of the x- and y-component of
the P vector. These variables are then used to calculate pattern strength
that is normalized to the pattern strength at $\theta=\phi=0$.

Assumptions

There are several assumptions built into the code which must be
recognized. The first is that this code models a parabolic reflector.
This is basic to the program and is not easily changed.

Several assumptions are made concerning the feed. It is assumed
to block a circular area (variable) at the center of the aperture and
produce a purely y-polarized field (the coordinate system used in the
computer code is the same as in the rest of this paper). Neither of
these parameters may be changed by specification from the files. The
feed is also assumed to produce a parabolically tapered electric field.
A wide range of aperture distributions may be approximated using this
formula and it is easily changed. Any function desired may be substituted
in the EFIELD function.

Use

The code accesses the files as listed following the two programs
to describe the antenna modeled and the far field points of interest.
The file ANTENNA lists all the parameters of the basic antenna, and the
file DISCS provides the parameters of the disc system. ANGLES controls
the far field points of interest and the number of these points.

The two programs differ in that MAIN1 reads the angles theta from
the file ANGLES and outputs both theta and the values of the summation
variables to the file PS. Program MAIN2 reads the values of theta from
the file PS along with the variables of summation. When program MAIN1
is run first for a given antenna system (and angle phi), it loads the
file PA with the appropriate values. Program MAIN2 may then be run with
different disc configurations. Since MAIN1 integrates over the entire
aperture and MAIN2 only over the discs (using the values of the summation
variables to calculate the value of the integral over the rest of the
aperture), MAIN2 requires a much shorter run time. The code, as written,
is a brute force integration technique, with no thinning as is commonly
employed in this type of program. (This was done to insure the discs'
effects were properly calculated.) Program MAIN2 is an attempt to provide
a much more efficient analysis tool. For the antenna analyzed in this
paper (the parameters of which are shown in the listing of the files
in this appendix), MAIN1 required approximately 8 cpu seconds to run
on a CDC Cyber 750 (a similar 6-foot dish required approximately 16 cpu
seconds). MAIN2, however, required only slightly over 1 cpu second to
run on the same machine with the two seven-inch discs (note that run
time for MAIN2 is controlled by disc size; a 6-foot dish would require

61

the same amount of time as a 4-foot dish if the area of the disc systems
of the two were equal).

Both programs output the pattern levels to the file PATTERN, and
to the terminal. (This assumes the programs are being run interactively;
if this is not the case, the deletion of the one output line will cancel
the terminal output.)

```
      PROGRAM MAIN1
      DIMENSION W(7),DX(7),DY(7),UAEF(2),XD(4),
     +YD(4),BP(4),DSHIFT(4),DISCR(4)
      REAL MN(4)
      DOUBLE PRECISION PXR,PXI,PYR,PYI
      OPEN(7,FILE='ANTENNA')
      OPEN(8,FILE='ANGLES')
      OPEN(9,FILE='DISCS')
      OPEN(10,FILE='PATTERN')
      OPEN(11,FILE='PS')
      DATA DX(1),DY(1),DY(2),DY(3)/4*0.0/
      DATA PXR,PXI,PYR,PYI/4*0.0/
      REWIND(7)
      REWIND(8)
      REWIND(9)
C     ANTENNA PARAMETERS READ
      READ(7,1000)SIDE,RADIUS,FREQ,F,BLOCK,C,N,PMAX,IDISC
 1000 FORMAT(/,6(/,E14.7,/),/I2,/,/,E14.7,/,/,/,I3)
C     FAR FIELD PLANE OF INTEREST (PHI) AND NUMBER OF
C     POINTS DEFINED
      READ(8,2000)PHI,NANG
 2000 FORMAT(/,/,F10.7,/,/,I3,/)
C     DISC PARAMETERS READ, AND CONSTANTS CALCULATED
      DO 50 IR=1,IDISC
      READ(9,2600)XD(IR),YD(IR),DISCR(IR),DSHIFT(IR)
 2600 FORMAT(3(/,E14.7,/),/,E14.7)
      DELTA=DSHIFT(IR)*3.0E+08/FREQ
      RP=SQRT(XD(IR)**2+YD(IR)**2)
      MN(IR)=-RP/(2.0*F)
      BP(IR)=(RP**2+4.0*F**2)/(2.0*RP)-
     +DELTA*(2.0*F-MN(IR)*RP)/(RP*SQRT(1.0+MN(IR)**2))
   50 CONTINUE
C     CONSTANTS FOR INTEGRATION SCHEME ARE ASSIGNED
      PIE=3.1415926535898
      BETA=2.0*PIE*FREQ/3.0E+08
      PHI=PHI*PIE/180.0
      W(1)=258.0/1008.0
      W(2)=125.0/1008.0
      W(3)=W(2)
      W(4)=W(2)
      W(5)=W(2)
      W(6)=W(2)
      W(7)=W(2)
      DX(2)=SIDE*SQRT(14.0)/5.0
      DX(3)=-DX(2)
      DX(5)=SIDE*SQRT(14.0)/10.0
      DX(7)=DX(5)
      DX(4)=-DX(5)
      DX(6)=DX(4)
      DY(4)=SIDE*SQRT(42.0)/10.0
```

63

```
        DY(5)=DY(4)
        DY(6)=-DY(4)
        DY(7)=DY(6)
        CPHI=COS(PHI)
        SPHI=SIN(PHI)
        YINCR=3.0*SIDE
        XINCR=SQRT(3.0)*SIDE
        N1=INT(RADIUS/XINCR).
C       FAR FIELD POINTS DEFINED (THETA)
        DO 700 L=1,NANG
        READ(8,3000)THETAD
  3000 FORMAT(F7.3)
        THETA=THETAD*PIE/180.0
        CTHETA=COS(THETA)
        STHETA=SIN(THETA)
        XC=XINCR/2.0
C       SUMMATION OVER THE APERTURE
        DO 600 IX=1,2*N1+1
        XC=-XC+XINCR/2.0
        IF (IX.EQ.1)XC=0.0
        ITEST=MOD(IX,2)
        IF (ITEST.GT.0) THEN
        YC=0.0
        YCC=0.0
        GO TO 300
        ELSE
        YC=YINCR/2.0
        YCC=YC
        GO TO 300
        ENDIF
   100 YC=YC+YINCR
        GO TO 300
   150 XC=-XC
        YC=YCC
        GO TO 300
   200 YC=-YC+YINCR
   300 CONTINUE
        IDTEST=0
C       POINT IS TESTED TO DETERMINE IF IT IS AFFECTED BY A DISC
        DO 350 ID=1,IDISC
        DIST=SQRT( (XC-XD(ID))**2+(YC-YD(ID))**2 )
        IF(DIST.LT.DISCR(ID)) GO TO 375
   350 CONTINUE
        IDTEST=2
   375 CONTINUE
        RPRIME=SQRT(XC*XC+YC*YC)
C       POINT IS TESTED TO DETERMINE IF IT IS ON APERTURE
        IF (RPRIME.LT.BLOCK) GO TO 100
        IF (RPRIME.GT.RADIUS) GO TO 550
```

```
C       INDIVIDUAL ELEMENT IS SUMMED OVER
        DO 500 I=1,7
        X=XC+DY(I)
        Y=YC+DY(I)
        RPRIME=SQRT(X*X+Y*Y)
        PHIP=ATAN2(Y,X)
        THETAP=2.0*ATAN(RPRIME/(2.0*F))
        CPP=COS(PHIP)
        SPP=SIN(PHIP)
        CTP=COS(THETAP)
        STP=SIN(THETAP)
        D=SQRT(1.0-SPP*SPP*STP*STP)
        UAEF(1)=(SPP*CPP*(1.0-CTP)/D)
        UAEF(2)=(SPP*SPP*CTP+CPP*CPP)/D
        C2=EFIELD(RPRIME,RADIUS,C,N)*W(I)
        ARG=BETA*RPRIME*STHETA*COS(PHI-PHIP)
        IF (IDTEST.EQ.0) THEN
        XP=(RPRIME-BP(ID))*MN(ID)
        S=SQRT(XP**2+RPRIME**2)+XP
        SHIFT=(2.0*F-S)*BETA
        ARGD=ARG-SHIFT
        PR=C2*COS(ARGD)
        PI=C2*SIN(ARGD)
        ELSE
        PR=C2*COS(ARG)
        PI=C2*SIN(ARG)
        ENDIF
        PXR=DPROD(PR,UAEF(1))+PXR
        PYR=DPROD(PR,UAEF(2))+PYR
        PXI=DPROD(PI,UAEF(1))+PXI
        PYI=DPROD(PI,UAEF(2))+PYI
  500 CONTINUE
  525 CONTINUE
        IF (YC.EQ.0.0) GO TO 200
        IF (YC.GT.0.0) THEN
        YC=-YC
        GO TO 300
        ENDIF
        GO TO 200
  550 IF (XC.GT.0.0) GO TO 150
  600 CONTINUE
C       FAR FIELD ELECTRIC FIELD (SQUARED) CALCULATED
        EVERT2=(PYR**2+PYI**2)*CTHETA**2
        EHOR2=(PXR**2+PXI**2)*CTHETA**2
C       PATTERN CALCULATED - NORMALIZED TO VALUE AT THETA=PHI=0
        PVERT=DB(EVERT2/PMAX)
        PHOR=DB(EHOR2/PMAX)
C       VARIABLES OF SUMMATION OUTPUT FOR USE IN PROGRAM MAIN2
        WRITE(12,4800)THETAD,PXR,PXI,PYR,PYI
 4800 FORMAT (F7.3,/,4(E40.33,/))
```

65

```
C       OUTPUT TO TERMINAL - MAY BE DELETEED IF NOT DESIRED
        WRITE (*,5000)THETAD,PVERT,PHOR,DSHIFT,PXR,PXI,PYR,PYI
C       ANTENNA PATTERN OUTPUT TO FILE PATTERN
        WRITE(10,5000) THETAD,PVERT,PHOR
 5000 FORMAT(7(F7.3,2X),/,4E10.3)
  650 CONTINUE
  700 CONTINUE
        STOP
        END
C       THIS FUNCTION ALLOWS ANY PARABOLICALLY TAPERED APERTURE FIELD
C       TO BE MODELED WITH PARAMETERS IN ANTENNA FILE.  MAY BE REPLACED
C       WITH ANY DESIRED ILLUMINATION
        FUNCTION EFIELD(R,RA,C,N)
        IF (N.EQ.0.0) THEN
        EFIELD=1.0
        GO TO 10
        ENDIF
        EFIELD=C+(1-C)*(1-(R/RA)**2)**N
   10 RETURN
        END
        FUNCTION DB(X)
        Y=ABS(X)
        IF (Y.GT.1.0E-08) GO TO 10
        DB=-80.0
        GO TO 20
   10 DB=10.3*ALOG10(Y)
   20 RETURN
        END
```

66

```
      PROGRAM MAIN2
      DIMENSION W(7),DX(7),DY(7),UAEF(2),XD(10),YD(10),BP(10)
     +,DSHIFT(4),DISCR(4)
      REAL MN(4)
      DOUBLE PRECISION PXR,PXI,PYR,PYI
      OPEN(7,FILE='ANTENNA')
      OPEN(8,FILE='ANGLES')
      OPEN(9,FILE='DISCS')
      OPEN(10,FILE='PATTERN')
      OPEN(11,FILE='PA')
      DATA DX(1),DY(1),DY(2),DY(3)/4*0.0/
      REWIND(7)
      REWIND(8)
      REWIND(9)
      REWIND(11)
      READ(7,1000)SIDE,RADIUS,FREQ,F,BLOCK,C,N,PMAX,IDISC
 1000 FORMAT(/,6(/,E14.7,/),/I2,/,/,E14.7,/,/,I3)
      READ(8,2000)PHI,NANG
 2000 FORMAT(/,/,F10.7,/,/,I3,/)
      DO 50 IR=1,IDISC
      READ(9,2600)XD(IR),YD(IR),DISCR(IR),DSHIFT(IR)
 2600 FORMAT(3(/,E14.7,/),/,E14.7)
      DELTA=DSHIFT(IR)*3.0E+08/FREQ
      RP=SQRT(XD(IR)**2+YD(IR)**2)
      MN(IR)=-RP/(2.0*F)
      BP(IR)=(RP**2+4.0*F**2)/(2.0*RP)-
     +DELTA*(2.0*F-MN(IR)*RP)/(RP*SQRT(1.0+MN(IR)**2))
   50 CONTINUE
      PIE=3.1415926535898
      BETA=2.0*PIE*FREQ/3.0E+08
      PHI=PHI*PIE/180.0
      W(1)=258.0/1008.0
      W(2)=125.0/1008.0
      W(3)=W(2)
      W(4)=W(2)
      W(5)=W(2)
      W(6)=W(2)
      W(7)=W(2)
      DX(2)=SIDE*SQRT(14.0)/5.0
      DX(3)=-DX(2)
      DX(5)=SIDE*SQRT(14.0)/10.0
      DX(7)=DY(5)
      DX(4)=-DX(5)
      DX(6)=DX(4)
      DY(4)=SIDE*SQRT(42.0)/10.0
      DY(5)=DY(4)
      DY(6)=-DY(4)
      DY(7)=DY(6)
      CPHI=COS(PHI)
      SPHI=SIN(PHI)
```

67

```
      YINCR=3.0*SIDE
      XINCR=SQRT(3.0)*SIDE
      N1=INT(RADIUS/XINCR)
      DO 700 L=1,NANG
      READ(11,3000)THETAD,PXR,PXI,PYR,PYI
 3000 FORMAT(F7.3,/,3(E40.33,/),E40.33)
      THETA=THETAD*PIE/180.0
      CTHETA=COS(THETA)
      STHETA=SIN(THETA)
      XC=XINCR/2.0
      DO 600 IX=1,2*N1+1
      XC=-XC+XINCR/2.0
      ITEST=MOD(IX,2)
      IF (ITEST.GT.0) THEN
      YC=0.0
      YCC=0.0
      GO TO 300
      ELSE
      YC=YINCR/2.0
      YCC=YC
      GO TO 300
      ENDIF
  100 YC=YC+YINCR
      GO TO 300
  150 XC=-XC
      YC=YCC
      GO TO 300
  200 YC=-YC+YINCR
  300 CONTINUE
      IDTEST=0
      DO 350 ID=1,IDISC
      DIST=SQRT( (XC-XD(ID))**2+(YC-YD(ID))**2 )
      IF(DIST.LT.DISCR(ID)) GO TO 375
  350 CONTINUE
      IDTEST=1
  375 CONTINUE
      RPRIME=SQRT(XC*XC+YC*YC)
      IF (RPRIME.LT.BLOCK) GO TO 100
      IF (RPRIME.GT.RADIUS) GO TO 550
      IF (IDTEST.GT.0)GO TO 525
      DO 500 I=1,7
      X=XC+DX(I)
      Y=YC+DY(I)
      RPRIME=SQRT(X*X+Y*Y)
      PHIP=ATAN2(Y,X)
      THETAP=2.0*ATAN(RPRIME/(2.0*F))
      CPP=COS(PHIP)
      SPP=SIN(PHIP)
      CTP=COS(THETAP)
      STP=SIN(THETAP)
```

68

```
          D=SQRT(1.0-SPP*SPP*STP*STP)
          UAEF(1)=(SPP*CPP*(1.0-CTP)/D)
          UAEF(2)=(SPP*SPP*CTP+CPP*CPP)/D
          C2=EFIELD(RPRIME,RADIUS,C,N)*W(I)
          ARG=BETA*RPRIME*STHETA*COS(PHI-PHIP)
          XP=(RPRIME-BP(ID))*MN(ID)
          S=SQRT(XP**2+RPRIME**2)+XP
          SHIFT=(2.0*F-S)*BETA
          ARGD=ARG-SHIFT
          PR=C2*COS(ARGD)
          PI=C2*SIN(ARGD)
          PRO=C2*COS(ARG)
          PIO=C2*SIN(ARG)
          PXR=DPROD(PR,UAEF(1))+PXR-DPROD(PRO,UAEF(1))
          PYR=DPROD(PR,UAEF(2))+PYR-DPROD(PRO,UAEF(2))
          PXI=DPROD(PI,UAEF(1))+PXI-DPROD(PIO,UAEF(1))
          PYI=DPROD(PI,UAEF(2))+PYI-DPROD(PIO,UAEF(2))
  500 CONTINUE
  525 CONTINUE
          IF (YC.EQ.0.0) GO TO 200
          IF (YC.GT.0.0) THEN
          YC=-YC
          GO TO 300
          ENDIF
          GO TO 200
  550 IF (XC.GT.0.0) GO TO 150
  600 CONTINUE
          EVERT2=(PYR**2+PYI**2)*CTHETA**2
          EHOR2=(PXR**2+PXI**2)*CTHETA**2
          PVERT=DB(EVERT2/PMAX)
          PHOR=DB(EHOR2/PMAX)
C         OUTPUT TO TERMINAL - MAY BE DELETED IF DESIRED
          WRITE(*,5000)THETAD,PVERT,PHOR,DSHIFT,PXR,PXI,PYR,PYI
C         ANTENNA PATTERN OUTPUT TO FILE PATTERN
          WRITE(10,5000) THETAD,PVERT,PHOR
 5000 FORMAT(7(F7.3,2X),/,4E10.3)
  650 CONTINUE
  700 CONTINUE
          STOP
          END
          FUNCTION EFIELD(R,RA,C,N)
          IF (N.EQ.0.0) THEN
          EFIELD=1.0
          GO TO 10
          ENDIF
          EFIELD=C+(1-C)*(1-(R/RA)**2)**N
   10 RETURN
          END
          FUNCTION DB(X)
          Y=ABS(X)
```

```
      IF (Y.GT.1.0E-08) GO TO 10
      DB=-80.0
      GO TO 20
10    DB=10.0*ALOG10(Y)
20    RETURN
      END
```

```
FILE=ANTENNA
SIDE (HEXAGON RADIUS)
.01
RADIUS (RADIUS OF THE APERTURE PLANE)
0.6096
FREQ (OPERATING FREQUENCY)
2.8E+09
F (FOCAL LENGTH OF DISH)
.6858
BLOCK (RADIUS OF AREA BLOCKED BY FEED)
.0762
C (FEED PARAMETER-ILLUMINATION AT EDGE OF DISH)
0.1
N (FEED PARAMETER-POWER OF PARABOLIC TAPER)
1
PMAX (NORMALIZATION VALUE FOR MAINDS)
5.7368911E+06
IDISC (NUMBER OF DISCS ON DISH)
0
```

71

X1
-0.2413
Y1
0.0
DISC RADIUS (DISCR)
0.0889
DFUNC1
0.2625
X2
0.2413
Y2
0.0
DISC RADIUS (DISCR)
0.0889
DFUNC2
0.260
X3
-0.1143
Y3
0.0
DISC RADIUS (DISCR)
0.03175
DFUNC3
0.306
X4
0.1143
Y4
0.0
DISC RADIUS (DISCR)
0.03175
DFUNC4
0.201

```
FILE=ANGLES
PHI (ANGLE THE PATTERN IS BEING TAKEN ACROSS)
00.0
NANG (NUMBER OF ANGLES THAT FOLLOW-(THETA) )
  4
THETA (ANGLE THAT THE PATTERN IS BEING COMPUTED FOR IN DEGREES)
10.0
11.0
12.0
13.0
```

EXAMPLE OF FILE PA AS GENERATED BY MAIN1T, AND USED BY MAINT2

```
    0.00
  .3381394382839149478594738018941700E-14
0.
  .23951807847187817798 73882437959820E+04
0.
    1.00
  .30848440323206796905777020762162720E-14
-.13193560979557438337326822212929490E-14
  .23091067709729478390215621451695500E+04
  .34720555910298240978199995580099100E-12
    2.00
  .22625486943082584835114493443010400E-14
-.23710637427334426357983921779371700E-14
  .20643189305137146626869054752060900E+04
  .56672013588103790868851432942050000E-12
    3.00
  .10988968266305436853382427225814500E-14
-.29531101297018878654688338858070300E-14
  .16983178658248567467077007C0388040E+04
  .63831109972142519850649436904762700E-12
    4.00
-.15260980723527219766406183200455210E-15
-.29766538842816927826189270255851400E-14
  .12649533186359215474684460986225500E+04
  .61126631813057532991185853035134200E-12
    5.00
-.12337632965914939445698395211429200E-14
-.24827957047449641911495879718979200E-14
  .82366831681248588266235353205054150E+03
  .27510529252991483599646628320453800E-12
    6.00
-.19444143937694776766748007028159900E-14
-.16250398805629524132287266778384000E-14
  .42825765032835392918644781435351100E+03
-.13332778858347677535011746594127050E-12
    7.00
-.21866037255893127707346312518298000E-14
-.62381162112040328300243156756334800E-15
  .11768340189879725729443078215504000E+03
-.60607900686094202574779748122149800E-12
    8.00
-.19791898597577371977167033935536800E-14
  .29298011322909018728260926192831100E-15
-.89127133999601263596400710935715020E+02
-.10979128957781593819314552454931900E-11
```

Bibliography

Abramowitz, Milton and Irene A. Stegun. Handbook of Mathematical
  Functions (Ninth Edition). New York: Dover Publications Inc.,
  1972.

Havens, Lt Douglas A. Pattern Nulling by Reflector Shaping.
  MS thesis, 83D-26. School of Engineering, Air Force Institute
  of Technology (AU), Wright-Patterson AFB OH, December 1983.

Jacavanco, Daniel. "Controlled Surface Distortion Effects,"
  Proceedings of the 1984 Antenna Applications Symposium.
  Robert Allerton Park, University of Illinois, 1984a.

-----. Telephone interview. Electromagnetics Technology Applications
  Section, Rome Air Development Center, Hanscom AFB MA,
  30 August 1984b.

-----. "Adaptive Reflectors." Current work briefing to AFIT personnel.
  Rome Air Development Center, Hanscom AFB MA, 20 March 1984c.

Lang, Jeffrey H. and David H. Staelin. "Electrostatically Figured
  Reflecting Membrane Antennas for Satellites," IEEE Transactions
  on Automatic Control, AC-27: 666-670 (June 1982).

Ludwig, Arthur C. "The Definition of Cross Polarization," IEEE
  Transactions on Antennas and Propagation, AP-21: 116-119
  (January 1973).

Silver, Samuel, Ed. Microwave Antenna Theory and Design. New York:
  McGraw-Hill Book Company, 1949.

Stutzman, Warren L. and Gary A. Thiele. Antenna Theory and Design.
  New York: John Wiley and Sons, Inc., 1981.

VITA

Captain Michael D. Rudisill was born on 15 February 1954 in Bloomington, Illinois. He graduated from Deland-Weldon High School in Deland, Illinois, in 1972 and attended the University of Illinois from which he received the degree of Bachelor of Science in Electrical Engineering in May 1976. Upon graduation, he received a commission in the USAF through the ROTC program. He completed pilot training and received his wings in May 1978. He then served as a B-52 pilot in the 20th Bombardment Squadron, Carswell AFB, Texas, until entering the School of Engineering, Air Force Institute of Technology, in May 1983.

Permanent address: 1401 Bird Court

Normal, IL   61761

REPORT DOCUMENTATION PAGE

1a. REPORT SECURITY CLASSIFICATION		1b. RESTRICTIVE MARKINGS			
UNCLASSIFIED					
2a. SECURITY CLASSIFICATION AUTHORITY		3. DISTRIBUTION/AVAILABILITY OF REPORT			
2b. DECLASSIFICATION/DOWNGRADING SCHEDULE		Approved for public release; distribution unlimited			
4. PERFORMING ORGANIZATION REPORT NUMBER(S)		5. MONITORING ORGANIZATION REPORT NUMBER(S)			
AFIT/GE/ENG/84D-55					

6a. NAME OF PERFORMING ORGANIZATION	6b. OFFICE SYMBOL (If applicable)	7a. NAME OF MONITORING ORGANIZATION
School of Engineering	AFIT/ENG	
6c. ADDRESS (City, State and ZIP Code)		7b. ADDRESS (City, State and ZIP Code)
Air Force Institute of Technology Wright-Patterson AFB, Ohio 45433		

8a. NAME OF FUNDING/SPONSORING ORGANIZATION	8b. OFFICE SYMBOL (If applicable)	9. PROCUREMENT INSTRUMENT IDENTIFICATION NUMBER			
8c. ADDRESS (City, State and ZIP Code)		10. SOURCE OF FUNDING NOS.			
		PROGRAM ELEMENT NO.	PROJECT NO.	TASK NO.	WORK UNIT NO.

11. TITLE (Include Security Classification)
Null Generation Using Discs on a Reflector

12. PERSONAL AUTHOR(S)
Michael D. Rudisill, B.S., Captain, USAF

13a. TYPE OF REPORT	13b. TIME COVERED		14. DATE OF REPORT (Yr., Mo., Day)	15. PAGE COUNT
MS Thesis	FROM _____	TO _____	1984 December	86

16. SUPPLEMENTARY NOTATION

17. COSATI CODES			18. SUBJECT TERMS (Continue on reverse if necessary and identify by block number)
FIELD	GROUP	SUB. GR.	Antenna, Directional Antenna, Parabolic Antennas
09	05		
14	02		

19. ABSTRACT (Continue on reverse if necessary and identify by block number)

Thesis Chairman: Andrew J. Terzuoli, Ph.D.

Approved for public release: IAW AFR 190-17.
LYNN ...
Dean for ... Professional Development
Air Force Institute ... ny (AIC)
Wright-Patterson AFB OH ...

20. DISTRIBUTION/AVAILABILITY OF ABSTRACT	21. ABSTRACT SECURITY CLASSIFICATION	
UNCLASSIFIED/UNLIMITED ☒ SAME AS RPT. ☐ DTIC USERS ☐	UNCLASSIFIED	
22a. NAME OF RESPONSIBLE INDIVIDUAL	22b. TELEPHONE NUMBER (Include Area Code)	22c. OFFICE SYMBOL
Andrew J. Terzuoli, Ph.D.	(513) 255-3576	AFIT/ENG

DD FORM 1473, 83 APR   EDITION OF 1 JAN 73 IS OBSOLETE.

It has been shown possible experimentally to produce nulls in the pattern of prime focus reflector antenna using discs mounted on the dish. A model of this antenna system is developed to evaluate optimal configurations and ideal performance.

Aperture integration is the method of analysis used. Discs' effects are modeled as a phase shift on the aperture. No secondary effects, such as diffraction, are considered.

Based on the model developed, guidelines are presented for antenna design. Computer code was written to implement the model and a prediction of an antenna system's performance is presented.

END

FILMED

4-85

DTIC